ADDIS ABABA UNIVERSTIY

INSTITUTE OF TECHNOLOGY

SCHOOL OF MECHANCAL AND INDUSTRIRAL ENGINEERING

Master of Science in Mechanical Engineering

(Under Railway Engineering)

DEVELOPMENT OF AN EFFECTIVE INSPECTION AND MAINTENANCE STRATEGYBASED ON ROLLING CONTACT SURFACE CRACK PROPAGATION ANALYSIS

By

Iyoel Chuchu

A Thesis Submitted To the Graduate School of Addis Ababa University in Partial Fulfillment of the Requirements for the Degree of Masters of Science

Advisor

Mr.Habtamu Tkubet

2017

ADDIS ABABA UNIVERSTIY

INSTITUTE OF TECHNOLOGY

SCHOOL OF MECHANCAL AND INDUSTRIRAL ENGINEERING

DEVELOPMENT OF AN EFFECTIVE INSPECTION AND MAINTENANCE STRATEGY BASED ON ROLLING CONTACT SURFACE CRACK PROPAGATION ANALYSIS

Mr.HabtamuTkubet (Msc)

Advisor	Date	Signature
Internal examiner	Date	Signature
External Examiner	Date	Signature
Dean/ Head	Date	Signature

DECLARATION

I hereby declare that the work which is being presented in this thesis entitled "**Development of an Effective Inspection and Maintenance Strategy Based on Rolling Contact Surface Crack Propagation Analysis**" is original work of my own, has not been presented for a degree in any other university; and that all sources of material used for the thesis have been duly acknowledged.

Iyoel Chuchu		
Name	Date	Signature

ACKNOWLEDGMENT

First of all I want to thank the almighty God for all his help in all my work including this thesis.

I would like to express my special thanks to my advisor Mr.Habtamu Tkubet for his invaluable advices that helped me out many times throughout every stage of the study.

I would like to express my heartfelt appreciation and gratitude to my mother for her patience, love, ideal supports to strengthen and enlightening vision. I would also like to thank all of my colleagues and class mates.

Finally, I appreciate the support from Ethiopian Railway Corporation (ERC) and Addis Ababa Institute of Technology (AAIT).

ABSTRACT

The issue of railway rail damage can't be seen easily and it requires attention and researching because most railway accidents are caused by the wheel/rail damage. The aim of this paper is to develop an effective inspection and maintenance strategy based on rolling contact surfaces crack propagation analyse. This will help to prevent the occurrence of rail failure by taking the required action at the right time, and extend the rail life expectancy, reduce the rail maintenance work and its cost.

The frequency of rail inspection tends to vary from one railroad to another, yet it is usually based on either time or traffic tonnage. Railroad companies have evolved their rail inspection schedules empirically based on long field experience. Rail defect management refers to the development and implementation of strategies to control the risk of rail failure. The primary method to control the risk is a rail inspection through non-destructive evaluation and, is a replacement of rails based on the remedial action plan.

This work has undertaken the study of fatigue cracks in rails using Finite element method (FEM) modelling and analytical solutions to provide rail inspectors for the quick assessment of the severity of surface breaking and embedded cracks in rails. The work does investigate crack propagation phenomena on the heads of rails.

Based on the analysis results, the mechanism for remedial action is developed based on critical crack size at rail head, to help infrastructure manager's decision. Then, effective number of rail inspection frequency is determined as three times a year to prevent the occurrence of rail failure by taking the required action at the right time, and extend the rail life expectancy, reduce the rail maintenance work and its cost. Finally, appropriate rail inspection and maintenance strategy model (flowchart) is adopted for Ethiopian railway industry.

Key words: Finite element method, linear elastic fracture mechanics, stress intensity factor, inspection and maintenance strategy

Table of Contents

LIST OF FIGURES

LIST OF TABELS

NOTATION

NDT	Non-destructive testing
LEFM	Linear elastic fracture mechanics
SIF	Stress intensity factor
ΔK	Range of stress intensity factor
K_I	Mode I Stress intensity factor
da_o/dN	Crack Growth rate
$f_i(\theta)$	Function that represents, stress dependence on θ.
a	Contact length in the major semi axis of ellipse
b	Contact length the minor axis of ellipse
a_c	Crack length in the major semi axis of ellipse
b_c	Crack length in the minor axis of ellipse
N	Number of load (Stress) Cycles
a_i	Initial crack size,
a_{ch}	Critical crack size at rail head
a_{cw}	Critical crack size at rail web
a_{cb}	Critical crack size at rail base
p_o	Maximum wheel-rail contact pressure
W	Design wheel load
E^w	Modulus of Elasticity of Wheel
E^r	Modulus of Elasticity of rail
v^w	Poisson's ratios of wheel
v^r	Poisson's ratios of rail

R_1^w	Principal rolling radii of wheel
R_1^r	Principal rolling radii of rail
R_2^w	Transverse radius of curvature of wheel
R_2^r	Transverse radius of curvature of rail
φ	Yaw rotation angle (The angle of the orientation difference of the principle axes of the two bodies)
Φ	Dimensionless impact factor (always>1)
Y	Geometric correction factor
M and n	Hertz coefficients
Δσ	tensile stress range
K_{IC}	Fracture toughness
No	Crack initiation period

CHAPTER ONE: - INTRODUCTION

1.1 Background of the Research

Railway infrastructure maintenance is of crucial importance in order to obtain a well-functioning transportation system. The actual maintenance work consists of a large amount of different activities, requiring considerable resources and large budgets. The European countries are reported to allocate 15 - 25 billion EUR annually on maintenance and renewals for a railway system consisting of about 300 000 km of track, half of which is electrified, giving an average of70 000 EUR per km track and year[1].

Currently, railways around the world employ track circuit based signalling systems that provide two important safety functions: a primary function of providing basic traffic flow regulation, and a secondary function of avoiding derailments by detecting broken rails ahead. Even though the conventional track circuit based techniques have been useful in reducing the risk of broken rail derailments and served the interests of the rail industries well, they are not accurate enough, and do not detect a substantial percentage of rail breaks in which electrical continuities are maintained[1].

Further, there exist dark territory rail lines, where the railway signalling equipment does not exist; in these low traffic sections, track circuitry is solely maintained for broken rail detection, although partial rail breaks that pose extreme severe derailment risks cannot be detected. Furthermore, joint bars in these track circuitries are vulnerable to breakage as much as the continuously welded rails (CWRs). Thus, the track circuitries are regarded as expensive, considering their limited contribution to broken rail detection and their own poor structural integrity, especially under heavy axle loading. In dark territories, manual interventions and restricted traffic control are the primary means of detecting broken rail or joint bars to maintain safety. This operational procedure often affects the overall productivity and performance of railway operations.

Actually railway construction in our country is also a main task to develop or to strengthen the transportation sector and to meet the country’s National Growth and Transformation plan. According to this plan besides to other types of constructions, railway is one of the main construction activities getting major emphasis in the transportation sector.

1.1.1Railway Track Structure

Rail transport refers to the land transport of people or goods along guided paths. A railway consists of two parallel rail tracks at a fixed distance (gauge) apart, usually made of steel and mounted upon cross beams called ties or sleepers as shown figure 1.1. A railroad consists of two steel rails which are held a fixed distance apart on a roadbed. Vehicles, guided and supported by flanged steel wheels and connected into trains, are propelled as a means of transportation.

The upper part consists of two parallel steel rails, anchored perpendicular to members called ties (sleepers) of timber, concrete, steel, or plastic to maintain a consistent distance apart, or gauge. The track guides the conical, flanged wheels, keeping the vehicles on the track without active steering and therefore allowing trains to be much longer than road vehicles [2].

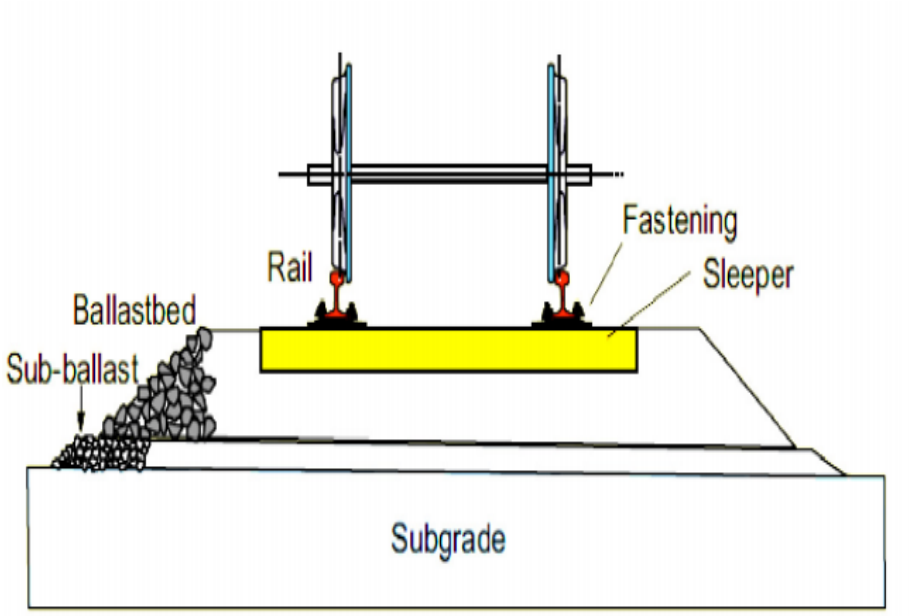

Figure1.1: Basic elements of a railway track [5]

1.1.1.1 Rail

Rail guides the conical, flanged wheels, keeping the vehicles on the track without active steering and therefore allowing trains to be much longer than road vehicles. The Characteristics of rail are rigidity, tenacity, hardness, and roughness of top surface [3].

The main function of rail is to supports the loads of vehicles (cars) and locomotives and guides their movements. The excellence of the track determines the permissible wheel loads, speeds; safety and dependability of railroad operation.it will support and guide the

wheels,provide a surface with smaller resistance, bear the force of the wheels and spread it to sleeper. No modern railroad can hope to survive in a competitive economy if its track is a hindrance to safe, dependable, on-time service. The rail used as track circuit in electrified railways and automatic block segments. A rail is hot rolled steel of a specific cross sectional profile (an asymmetrical I-beam) designed for use as the fundamental component of railway track.It is composed of rail head, rail web and rail base. The rail head and base must be large and thick. [3]

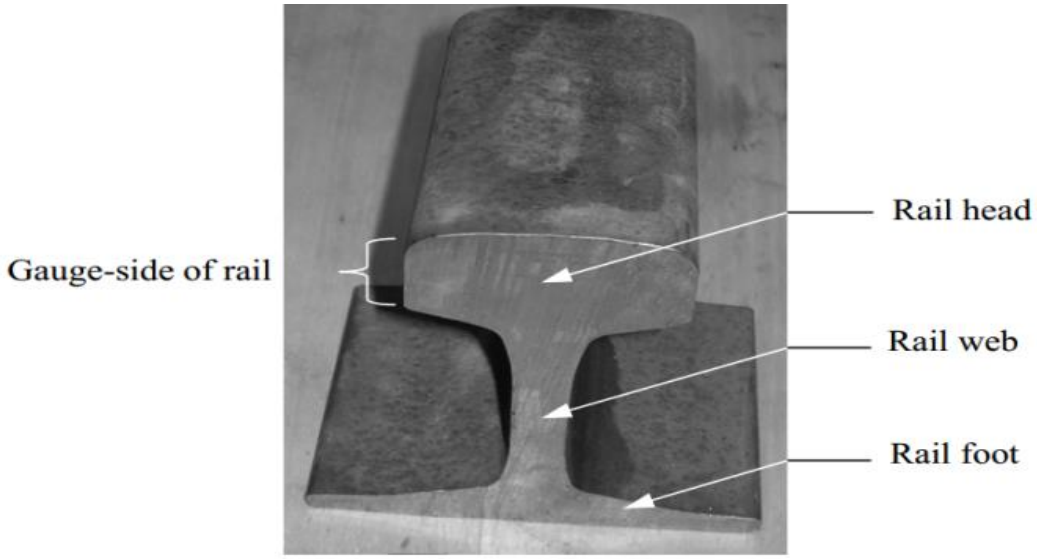

Figure1.2: Flat bottom Rail profile [3].

1.1.1.1.1Types of Rail

Determining factor for rails strength and hence axle loads and speeds is weight of a rail per length. So rail types are divided by its unit weight in China, such as 75, 60, 50, 43 kg/m. Standard rail length are 12.5m and 25m [3].

The following rail forms are in use at present:

- *Vignola's* rail (standard railway rail with head, web and foot),
- Double-head rails with head, web and foot (obsolete)
- Grooved rails for tram ways,
- Switch rails and
- Crane rails etc.

1.1.1.1.2 Rail Requirement

The rail is running surface, carrier and guiding element at the same time. It is subject to equal static and dynamic stress. In heavy haul traffic, axle loads up to 35t are applied. Depending on the topography rails are laid with radii as low as 300m, therefore, they have to bear very high lateral forces exerted by the wheel flange striking against the gauge corner of the outer rail.

To be able to withstand manifold and high forces, the rails must meethigh resistance to wear, high resistance to compression, high resistance to fatigue, high yield strength, tensile strength and hardness, high resistance to brittle fracture, good weld ability, and high degree of purity, good surface quality and low residual stress after manufacturing [3].

1.1.1.1.3 Method of joining rail section

Railway rails are manufactured in sections of 25- 120 m length which are joined in track by bolting or welding. Two advantages with welded rail sections in contrast to bolted ones are the lower maintenance cost and the improved dynamic behaviour of the train-track-rail system. There are primarily two rail welding processes which are used today, the flash-butt welding and alumino-thermic (thermite) welding processes.

Whereas the thermal stresses, at temperatures deviating from the rail neutral temperature at which the track was installed, in the old designs were concentrated at the fish bolts and rail ends as the weakest links, they now affect the entire rail length in welded tracks. Sometimes, when track circuits are used for signalling purposes, insulation joints are used even in continuously welded tracks. In order to compensate the loss of strength due to the insulated block, side plates similar to the fishplates fastened by epoxy resin are used[4].

A rail is hot rolled steel of a specific cross sectional profile (an asymmetrical I-beam) designed for use as the fundamental component of railway track. Continuous welded track (CWR) are welded into 100-200m long rail in factory, and then be welded again into1000-2000m long rail in the laid place within 25 m of rail. Continuous welded track (CWR) has smooth driving, low maintenance cost and long life advantages. Furthermore, joint bars in these track circuitries are vulnerable to breakage as much as the continuously welded rails (CWRs). Rail gaps are used to adapt to the needs of expanding with heat and contracting with cold, the rail gap cannot too big or too small.

(a)

(b)

(c)

(d)

Figure1.3: Types Rail joints [38].

(a) Fishplate with bolts; (b) continuous (aluminothermy) welded rail; (c) fishplate joint of a broken rail; (d) defective isolation joint.

1.1.2**Train-Track Interaction**

The dynamic interaction between the train and the track determines the wheel–rail contact forces and the relative motion between wheel set and track. Many parameters influence the behavior: the mechanical properties of the track (including rails, rail pads, fasteners, sleepers, ballast and underground), the mechanical properties of the vehicle (including wheel sets, bogies and wagon primary and secondary suspensions), the conditions in the wheel–rail interface (including its geometrical, frictional and deformation properties) and also track alignment, curves, axle load and train speed. Stability against lateral oscillations (hunting) and curving performance are important aspects [2].

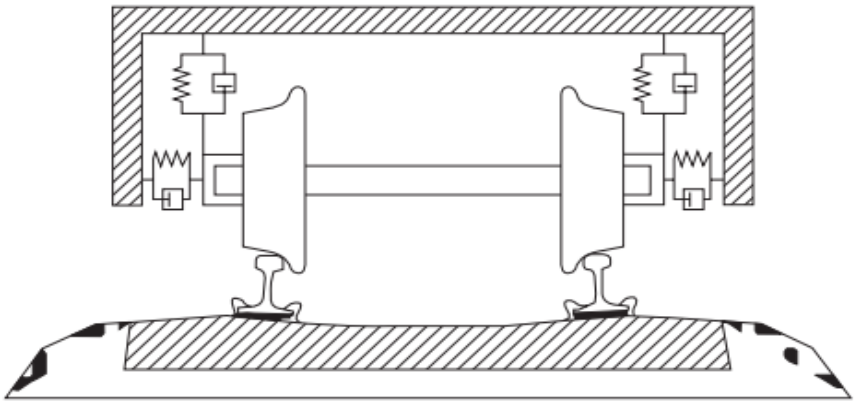

Figure1.4: Sketch of bogie with primary suspension and wheel set in contact with rails [2].

The wheel–rail contact forces may be indirectly measured by use of instrumented wheels or rails. There is no known operational method for direct measurement in the contact patch of the wheel–rail contact forces. Traction and braking impose additional shear forces, creep, sliding and thermal loading that are often crucial for the wheel–rail interface. Further, tread braking of the wheels may impose excessive heating, thermal cracking and corrugation of the wheel rim that will indirectly affect train–track interaction.

1.1.3The Wheel–Rail Interface

The high energy efficiency of railway transportation is made possible by the favorably low losses in the rolling contact between the hard surfaces of the wheel and rail, which meet only in a very small contact patch. However, several undesired phenomena may occur in this contact, vertical contact forces, but also lateral and longitudinal forces, induce stresses that may cause material yielding and fatigue. Rolling contact forces combined with friction induce wear.

Traction and braking may lead to wheel sliding, resulting in rail burns and wheel flats, unfavorable material phase transformations and thermal cracks. These phenomena may create irregularities and/or worn profile geometries of the wheel and rail, resulting in poor vehicle dynamics and a further increase in contact forces and in vibrations and noise. The consequence may be discomfort and disturbance for passengers and the surroundings and also increased maintenance costs for wheels and rails and other components. Severe cases can even result in derailment induced by wheel or rail fracture or by the wheel flange climbing on the rail [2].

(a) (b)

Figure1.5: Types of wheel rail contact [2].

(a) Wheel tread and rail ball contact (b) wheel flange root and rail gauge face contact

At typical wheel–rail interface in new or newly maintained condition and a wheel profile in worn condition. The original profiles often follow some standard or practice, depending on the application. A typical contact patch, for standard wheel and rail profiles in new condition and a vertical contact force of 11 tones, is elliptic with size 18 × 11 mm, longitudinally and laterally, respectively. For the worn profile, the contact patch will be more circular. The conicity of the wheel tread provides the steering capacity of the wheel set and is therefore important for the running stability of the wheel set and bogie. The rail inclination may be 1.5–3°, dependent on national practices [5].

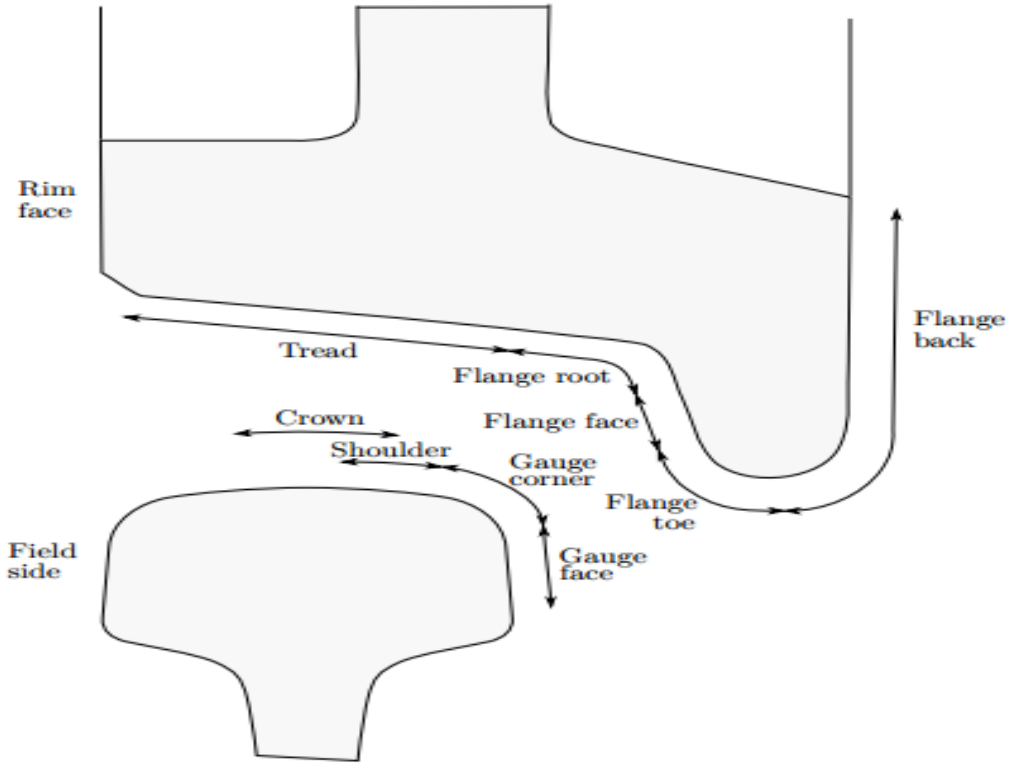

Figure1.6: Nomenclature of parts of the wheel rim and rail head [5].

1.1.4 Rail loading and stress at the Rail/Wheel Interface

1.1.4.1 Rail loading

1. **Vertical loading-** load forces applied by the wheel tread under normal train operation. They are normally characterized as static load, dynamic load, and impact load. Static load is the gross weight of the railcar divided by the number of wheels; static loading can be influenced by track curve super elevation. Dynamic loading is the increase in static load that results from train speed. Impact loading is the additional increased loading over static and dynamic loads that occur when a wheel travels over the head irregularly or the wheel contains a flat spot.
2. **Lateral loading-** load forces applied by the wheel flange to the high rail in curved track. In sharp curves, lateral loading is normally stable throughout the curve; however, in a shallow curve or tangent track, lateral loading may occur due to track hunting.
3. **Creep-** load forces that are generated at the rail/wheel interface by the rolling action of the wheel. Longitudinal creep results from traction applied by the wheel. Transverse creep results from lateral movement of the wheel during track hunting.

1.1.4.2 Rail Stresses

1. **Bending stress-** bending of the rail that occurs from vertical or lateral wheel loading. Vertical wheel loading results from loading between tie supports and causes tensile longitudinal stresses in the base and head/web fillet areas. Lateral wheel loading applies tensile longitudinal stresses in the web area and head/web area of the rail field side.
2. **Thermal stress-** occurs in continuous welded rails due to thermal expansion and contractions (when actual rail temperature increases above or below the rail neutral temperature). When the temperature is above, compressive longitudinal stresses occur. When the rail temperature is below, tensile longitudinal stresses occur. These stresses can drastically influence rail flaw development.
3. **Residual stress -** a result of the manufacturing process, particularly from roller straightening and head hardening. It can also result from the rail welding since expansion and contraction occurs during the weld process. Residual stresses can be found in any location within the rail section [5].

1.1.5 Fracture Mechanics

The term “fracture mechanics” refers to a vital specialization within solid mechanics in which the presence of a crack is assumed, and quantitative relations between the crack lengths, the material’s inherent resistance to crack growth, and the stress at which the crack propagates are defined .It deals with the behaviour of cracked bodies subjected to stresses and strains. These can arise from primary applied loads or secondary self-equilibrating stress fields [26].

Fracture mechanics based analyses have been performed for a number of simplified crack geometries some of which are summarised in Figure 1.7. Many investigations focussed on elliptical internal cracks (in North American sources also designated as “detail cracks” or “detail fracture”), shown in Figure 1.7a. Other transverse crack types such as straight and semi-elliptical surface cracks in the rail head Figure 1.7 c and d, and the rail foot shown in Figure 1.7 f and corner cracks at both sites shown in Figure 1.7 b, g, and d have also been investigated. Besides the transverse crack geometries further crack configurations such as web cracks induced by bolt holes and weldments, vertical axial rail head cracks (splits)and cracks in switches have been investigated as well [6].

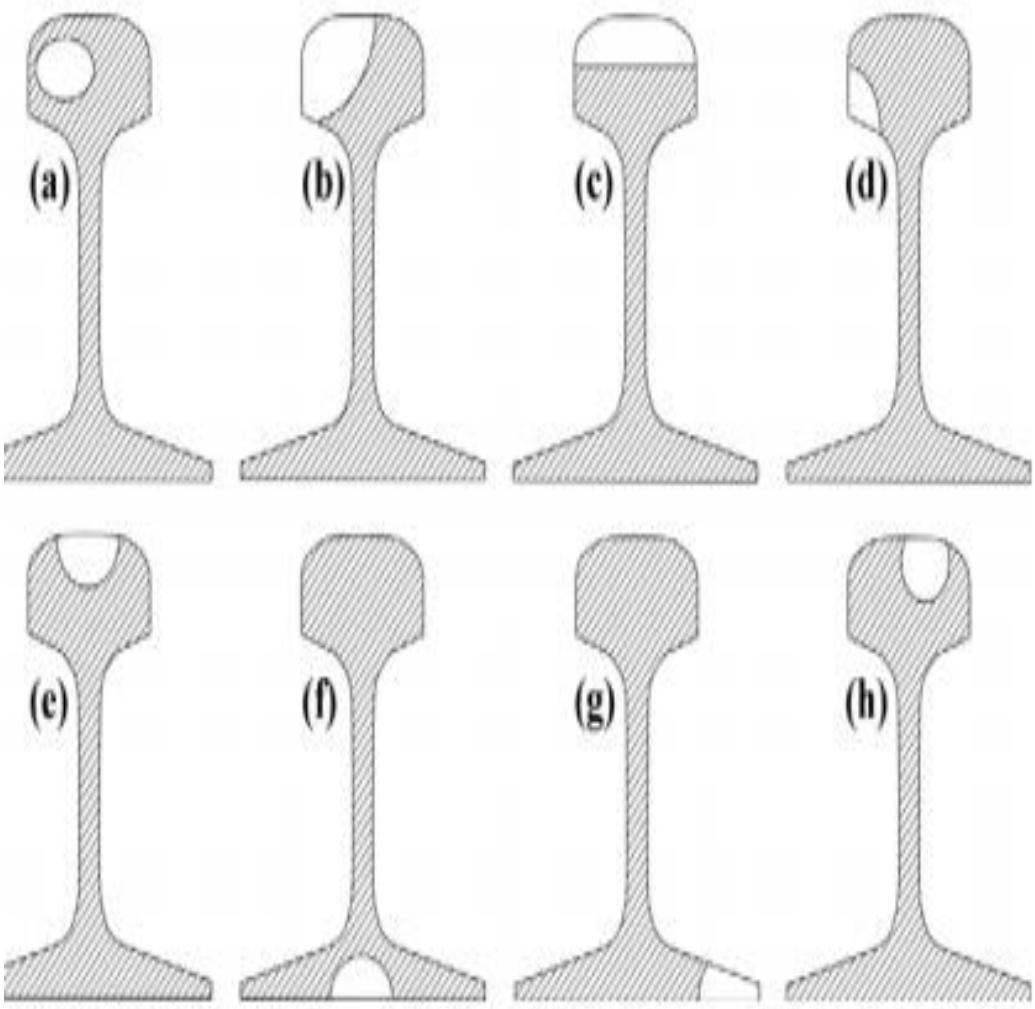

Figure1.7: Some crack configurations in rails [6].

1.1.5.1Common types of broken rails

Common types of broken rails are shown in figure 1.8 any breakage that occurs over the joint bars, rails or welds in any shape or form is classified as a broken rail incident; as can be seen, partly damaged, cracked or separated rails are also counted as incidents within the limits of the special track work, as they pose high risks to the safety of trains.

Rails are designed as beams resting on continuous elastic foundation. This theory assumes the beams as continuous; any break in rail changes this assumption, causing severe disruption to the deflections and rotations determined at design stage. Even a breakage far away from a wheel can potentially affect the rail rotations under the wheel that change the contact conditions, leading to undesirable dynamics for the wheel sets. The vibration signature of the rails can be used for the prediction of the damage levels including breakage [6].

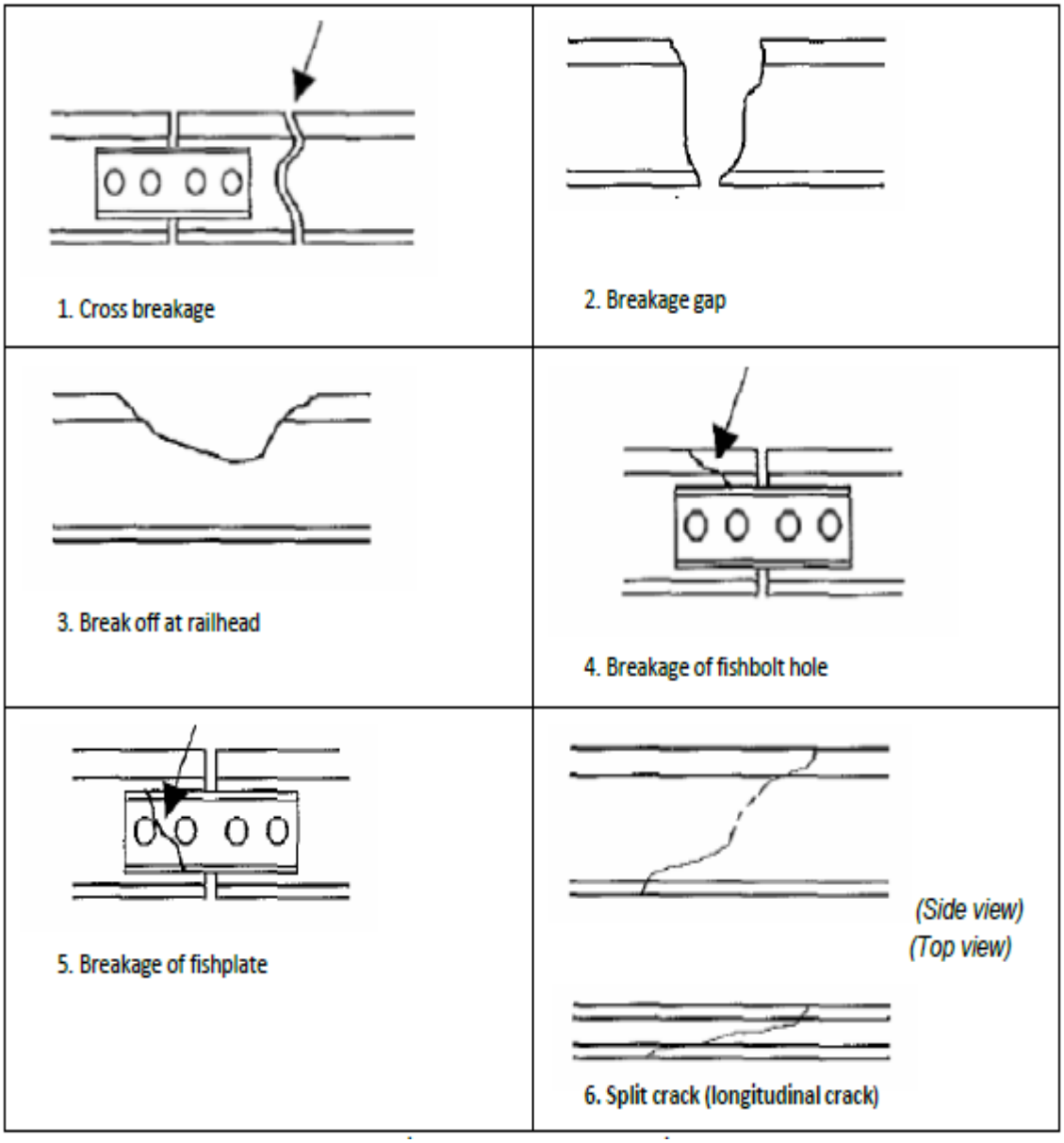

Figure1.8: Common types of rail break [6]

1.2 Research Problem Statements

Rails guide trains are subjected to severe contact stresses at the wheel–railhead interface. Each wheel passage reshapes the railhead profile due to wear; extreme levels of stress concentration also induce surface and subsurface fatigue cracks in railheads (Figure 1.9). Routine grinding and re-profiling save railheads from the growth of the initiated cracks to critical levels that lead to partial or full breakage of the rail. In spite of the fact that railway companies around the world have attempted to reduce the number of broken rails by making the use of various management techniques, the number have not yet reached zero and a substantial proportion of railway budget is spent on rail track inspection and maintenance [6].

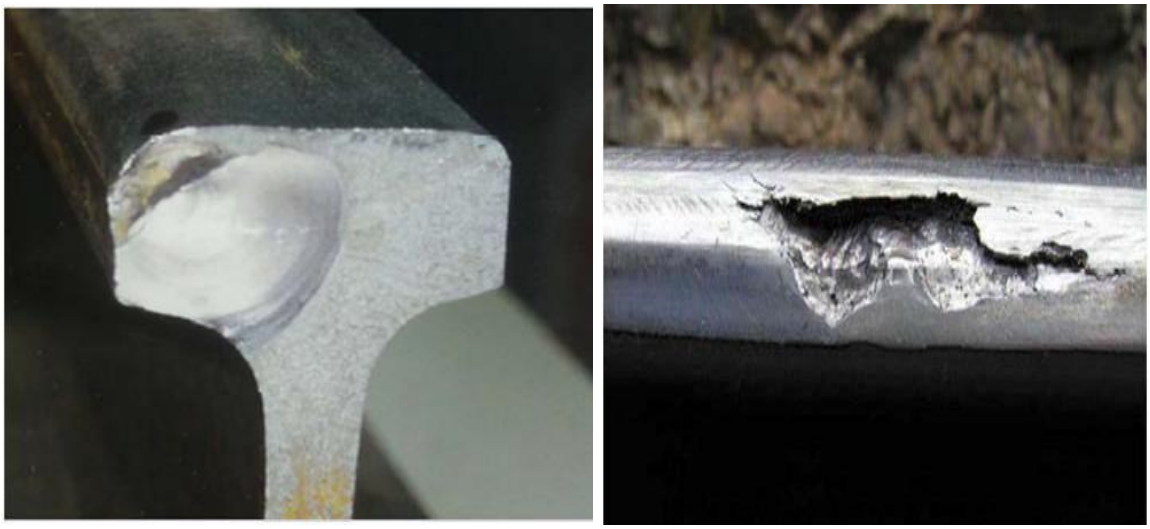

(a) (b)

Figure1.9: Typical examples of broken rails and rail damage [6].

A positive trend found with respect to the mentioned British network was that, whilst the detection rate of damaged rails which then had to be removed, the number of breakages was virtually constant (Figure 1.10). This fact shows that countermeasures, such as non-destructive inspection and periodical grinding, have brought a significant improvement towards failure prevention [7]. On the other hand, the requirements on the networks such as an increased volume of traffic and higher axle loads etc. are permanently increasing. Therefore, fatigue crack propagation in rails remains an important issue with respect to both the quantitative understanding of the mechanisms and the development of analysis routines for practical application.

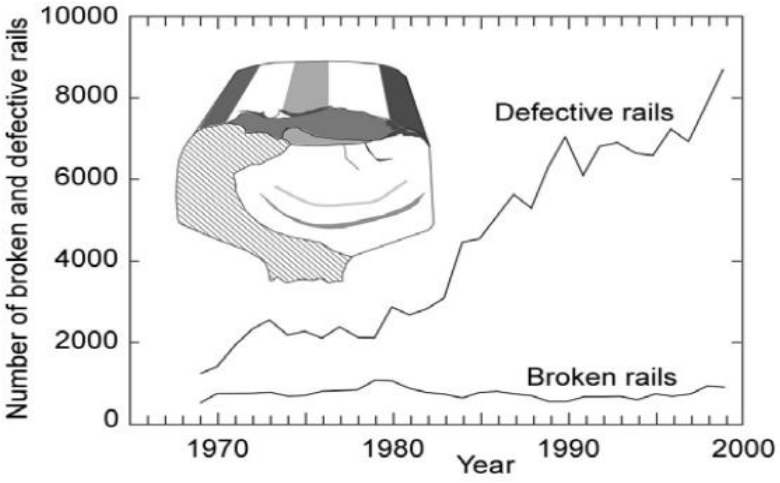

Figure1.10: Long term trend of broken and defective rails removed in rail track railroad network [7].

This problem exists in Ethiopian railway industry after operation starts due to:

- Rails deteriorate over the time due to vast movement of the people, huge import and export of goods with frequent cycle and needs maintenance to correct damage, deterioration, and cracks due to different factors which influence the rail degradation process.
- Ethiopian railway transport has no life time rail management technique developed for determination of the mechanism for remedial action of rails as well as effective rail inspection interval for the reduction of costly failure in the future as well as well-defined efficient and effective rail maintenance procedure (model).

1.3 Objectives of Research

1.3.1 General Objectives

The main objective of this research is to develop an effective inspection and maintenance strategy based on rolling contact surfaces crack propagation analyse. This will help to prevent the occurrence of rail failure by taking the required action at the right time, and reduce the rail maintenance work.

1.3.2 Specific Objectives

1) Describes information on crack types and the stages of rail fracture as well as the factors that have to be considered in modelling the damage behaviour of rails.
2) Analysis of rail stress and crack development process with finite element method FEM
3) Develop mechanism for assessment and remedial action for different rail crack which will help in decision making when planning future inspection and maintenance intervals and determine fatigue life of rail.
4) Adapt the efficient and effective rail inspection and maintenance procedure (flowchart).

1.4 Research Methodology

The research methodology for this study involved the following major tasks: literature review is performed to document the validation of the linear elastic fracture mechanics analysis for effective rail inspection and maintenance method. Following literature review, three step analyses is used for the determination of mechanism of remedial action of rails and effective rail inspection interval.

The methods applied in the thesis are depicted in the following steps

Step 1: Rail stress analysis

The contact surface and pressure between wheel and a rail would be determined by Hertzian contact theory. A rail is modelled by solidwork and inserting in to ANSYS 14.5 the rail stress and deformation can be determined. For information about rail design parameter, rails in National railway network of Ethiopia are employed.

Step 2: Predicts the fatigue life of rail linear elastic fracture mechanics.

By inserting a crack on the rail head surface With ANSYS 14.5 the stress intensity on a crack will be resulted. By using numerical method the critical crack size and number of cycle load with fatigue life of rail would be determined.

Step 3: The Frequency of Rail Inspection and Maintenance

The numbers of rail inspection per year can determine by using the maximum number of cycle.

Step 4: The damage identification techniques and the effective rail inspection with maintenance flow chart procedure (model) are involves.

Finally: Organization of the document.

CHAPTER TWO: - LITERATURE REVIEW

2.1Review of Rail surface Crack Types

2.1.1Rail Head Cracks with Surface Origin

Typical cracks originating at the running surface are the so-called “head checks” and “squats” [8].

2.1.1.1 Head checks

Head checks are groups of fine surface cracks at the running (gauge) corner of the rails with a typical interspacing of 0.5 to 10 mm. Their multiple occurrences make them particularly dangerous as has been demonstrated [8].

Head checking preferentially occurs at the gauge corner of the outer rail in curved tracks but is also found at switch or crossing rails. The reason is gross plastic deformation due to friction when the wheel passes. The cracks grow at a flat angle to the running surface in the traffic direction whereby lubrication plays an essential role [8]. They can cause spalling of pieces of material between the cracks (Figure 2.1) but also - after deviating at some millimetres of growth – causes transverse cracks leading to the eventual fracture of the rail.

(a) (b)

Figure2.1: Head checks defects [40].

a) Spalling originating at head checks’) Fracture of a rail with origin from a head check. (The rail was broken up in the laboratory.)

2.1.1.2 Squats

Like head checks squats are rolling contact induced defects. They occur in straight or slightly curved cracks, however, not at the gauge corner but at the running surface. In contrast to head checks they occur randomly at isolated sites [8]. Squats and head checks have in common that their existence is not associated with any metallurgical fault but are caused by gross plasticity.

Squats grow at a sharp angle with respect to the running surface until they turn into the transverse direction .They are visible at the surface as a widening of the rail/wheel contact band together with a small depression at the surface sometimes called "dark spot" (Figure 2.2).

Figure2.2 :Squat: damage of the running surface ("hot spot" and crack nucleation) [8].

One reason for more frequent occurrence of surface induced rail head cracks, particularly on high-speed tracks, are improvements in the wear resistance of modern rail steels. It should be noted that there is a competition between early fatigue crack propagation and metal removal due to wear.

2.1.2 Rail Head Cracks with Internal Origin

2.1.2.1 Kidney-shaped cracks

In former times rail cracks with internal origin rather than surface induced cracks, were dominating the failure statistics. This type of cracks usually initiates from manufacturing defects, e.g. hydrogen shatter cracks, so-called "flakes" (Figure 2.3a). The pre-existent flaw is the nucleus for a so-called "kidney-shaped crack or "tacheoval" (Figure 2.3 b). Note, however, that sub-surface cracks can also initiate in virtually defect-free material.

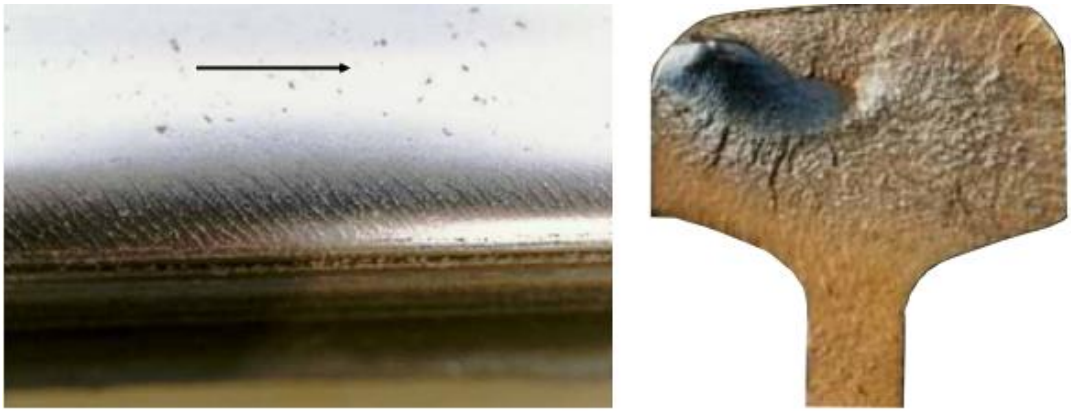

(a) (b)

Figure2.3: Kidney-shaped crack in a rail head [38].

(a)Transverse section of a rail head containing hydrogen shatter cracks ("flakes"). (b) "Kidney-shaped" crack in a rail head.

2.1.2.2 Longitudinal cracks

Special types of subsurface induced cracks are horizontal cracks beneath the gauge corner which can lead to breaking out of material (gauge corner shelling) but also to subsequent transverse crack propagation (so-called detail fracture). The latter starts at one or both ends of a surface "shell".

The crack origin is usually about 10 mm below the surface and associated with a band of non-metallic inclusions. Improved rail materials are the main reason why, at most railway companies today, rail head cracks with internal origin play a less important role compared to cracks with surface origin.

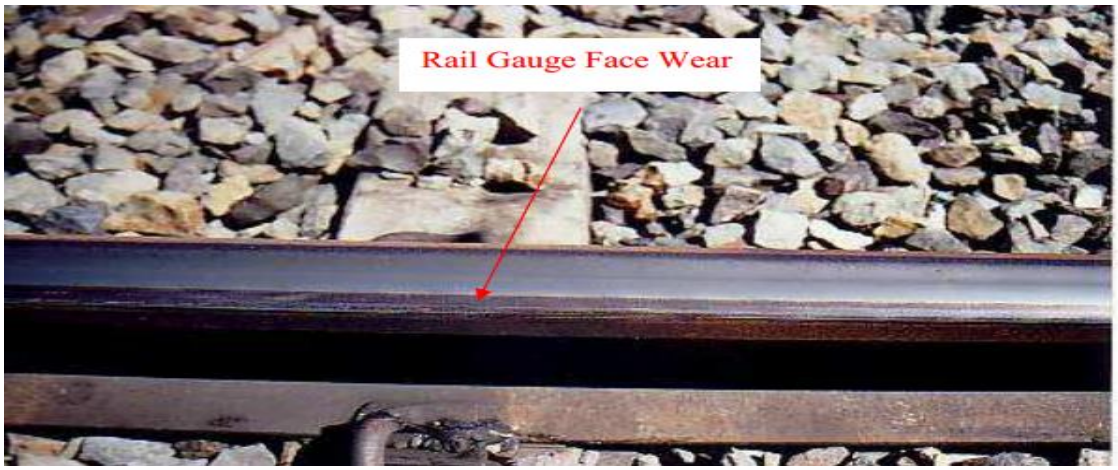

Figure2.4: Gauge corner shelling at an early stage [38].

2.1.3 Rail Web Cracks

2.1.3.1 Longitudinal vertical and horizontal cracks

Cracks in the web are usually caused by poor manufacturing. One example is the longitudinal vertical crack (Figure 2.5a) also known as "piping". A horizontal crack and the branching at its end is shown in Figure 2.5b. Both types of web cracks will lead to rail fracture.

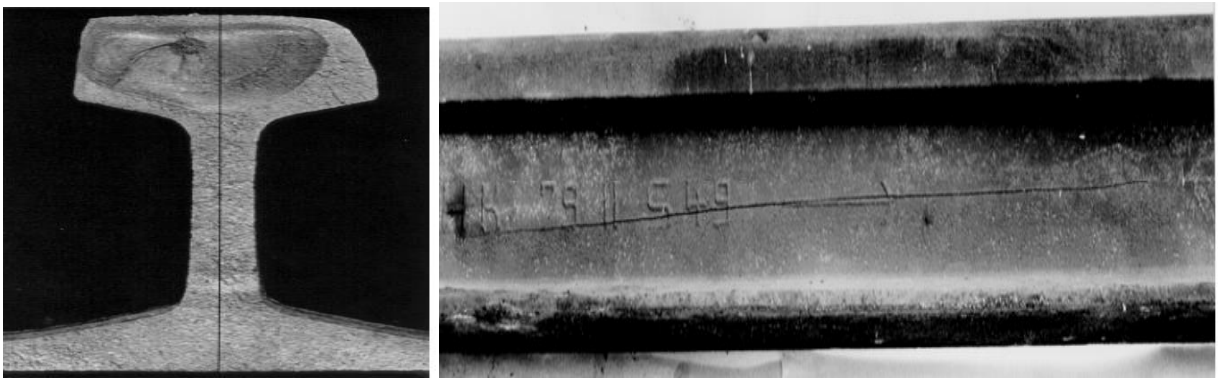

(a) (b)

Figure2.5: web cracks [38].

(a) Longitudinal vertical web crack ("piping"), (b) Horizontal web crack.

2.1.3.2 Cracks initiated at machined holes in the web

Machined holes can be fishbolt holes used for joining the rails instead of welding but also holes for insulation joints. Initially, the cracks usually grow at an angle of about $45^0$to the horizontal, but can change their direction at further extension (Figure 2.6). When crack initiation is caused by vertical stresses due to fishplate restraint, cracks can also grow at an angle of 0^0as can be seen in the figure. Cracks initiating at holes are particularly dangerous when they occur near the rail ends as in the case of fishbolt holes.

Figure2.6: Web cracks originating from a fishbolt hole [16].

2.1.4 Rail Foot Cracks

2.1.4.1 Transverse rail foot cracks

Rail foot cracks can be transverse or longitudinal. Transverse cracks are usually initiated from galling due to wear and/or corrosion at the rail support. Since they are hard to detect they will frequently cause fracture [8].

2.1.4.2 Longitudinal rail foot cracks

In contrast to the transverse foot cracks the reason for the occurrence of this type of defects is poor manufacturing. Two types of longitudinal foot cracks can be distinguished with respect to their location in the foot. If the foot crack is away from the centre line of the foot it will probably cause a piece of the foot to break away. However, if it is near the centre part complete fracture of the rail can be the consequence. An example of a longitudinal crack is provided in Figure 2.7 [8].

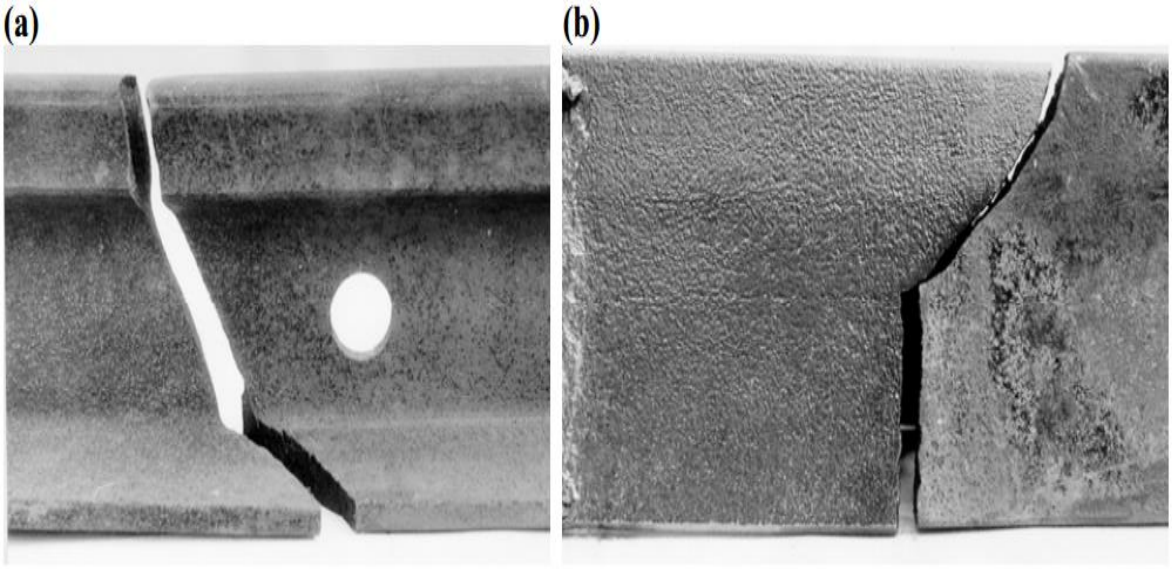

Figure2.7: Fracture due to a longitudinal foot crack [8].

(a) Side view; (b) foot underside.

2.1.5 Cracks at welds and switches

Meißner and Hug [9] evaluated statistical data of 65,000 kilometres track including 89,000 switches in Germany. They found that 34% of the rail fractures or detected cracks belonged to welds compared to 66% for the rest of the track and that 23% concerned switches compared to 77 % for other track positions. The statistics shows that both welds and switches require special attention with respect to their damage tolerance behaviour.

2.1.5.1 Cracks at Welds

The most common used rail welding methods today are flash-butt welding and aluminothermy or thermite welding. According to Skyttebol [10] the failure rate of thermite welds is 10 times as high as that of flash-butt welds. Nonetheless thermite welds are used world-wide for welding in the field. There is a modification of the material properties (particularly the toughness) on a local scale.

- There are at least three effects which affect the nucleation and growth of cracks in or near welds.
- Welding residual stresses are induced which act as loading components on a pre-existing crack but can also contribute to the nucleation of cracks during the joining process or later on.
- Residual distortions from the joining process affect the straightness and alignment of the rails which influence the dynamic load magnification during train passage.

Since the material at the running surface, and some millimetres beneath, is strongly deformed and compression residual stresses are generated in that region, and since the global bending stresses are highest in the foot, fatigue cracks in welded rails tend to grow from underneath rather than from the rail head (Figure 2.8).

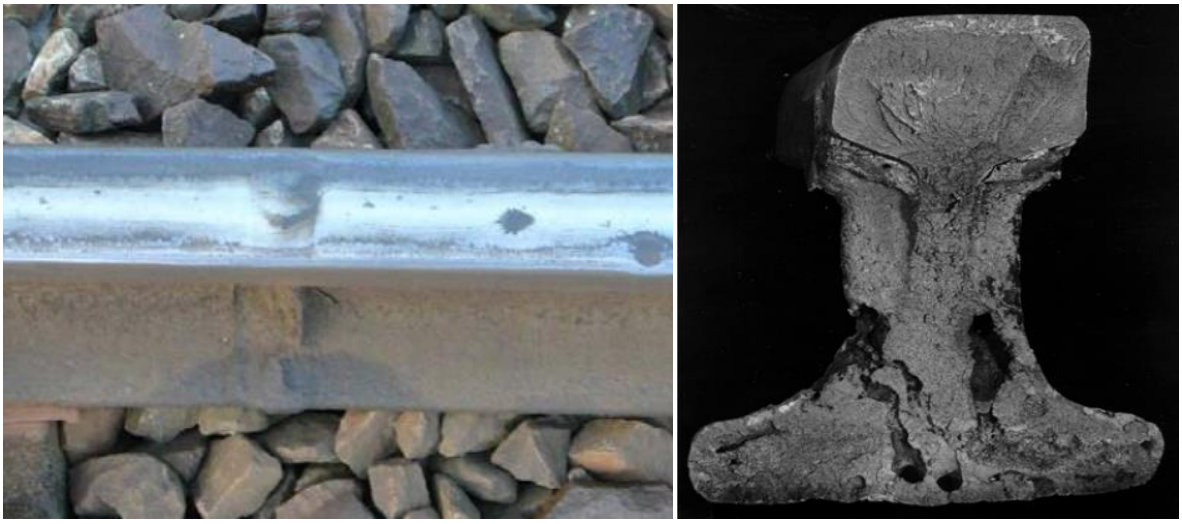

(a) (b)

Figure2.8: welded rails crack and fracture [10].

(a) Fatigue cracks in welded rails (b) Fracture of an alumino-thermite weld due to weld defects in the foot.

2.1.5.2 Cracks at Switches

Cracks at switches are similar to cracks on the straight track. Their origin and extension will, however, be affected by the geometrical features of the switch rails. Note that a preferred crack initiation site is the rail section where the stress induced by the lateral bending moment reaches its maximum due to the reduced rail foot width.

(a) (b)

Figure2.9: Rail foot crack and fracture [38].

(a) RCF damage at the transition to the nose (right, zoom-in); (b)Fracture of rail caused by a crack which initiated at a cut out at the foot underside.

2.2. Review of Rail Surface Crack Stages

2.2.1 Crack Initiation

2.2.1.1 Nucleation and Initiation Process

The squat-like cracks on top of the railhead considered here are caused by large and alternating plastic strains close to the railhead surface. The strains are induced by normal and shear contact stresses from the rolling wheel of the Hertzian type and by roughness-related local high stresses.

Residual stresses formed by plastification will suppress further plastification. The initiation could start at the surface or at a subsurface position depending on the loading, although squat-like cracks normally initiate at the surface and propagate into the rail at a shallow angle to the surface. The hydrostatic stresses (compressive) mean that material imperfections will have less influence on the fatigue life than in a conventional fatigue problem [11].

2.2.2 Crack Propagation

2.2.2.1 Early Crack Growth in Rails

Repeated rolling contacts cause rolling contact fatigue (RCF) and wear on the railhead. High tangential forces together with surface roughness induce uniaxial plastic deformations in a thin surface layer. Surface breaking cracks are then initiated on the top of the rail (squat & rail fracture) or at the gauge corner. Once a crack has been initiated (with a length of, say, 0.1 mm) it will grow at a shallow angle (10-25^0) from the surface in the direction of the plastically deformed anisotropic material until it reaches a critical length (of, say, 1-2 mm), see Figure 2.18. At this critical length the stresses and strains at the crack tip will govern the continued growth which can be upwards (spall) or downwards (squat) [12].

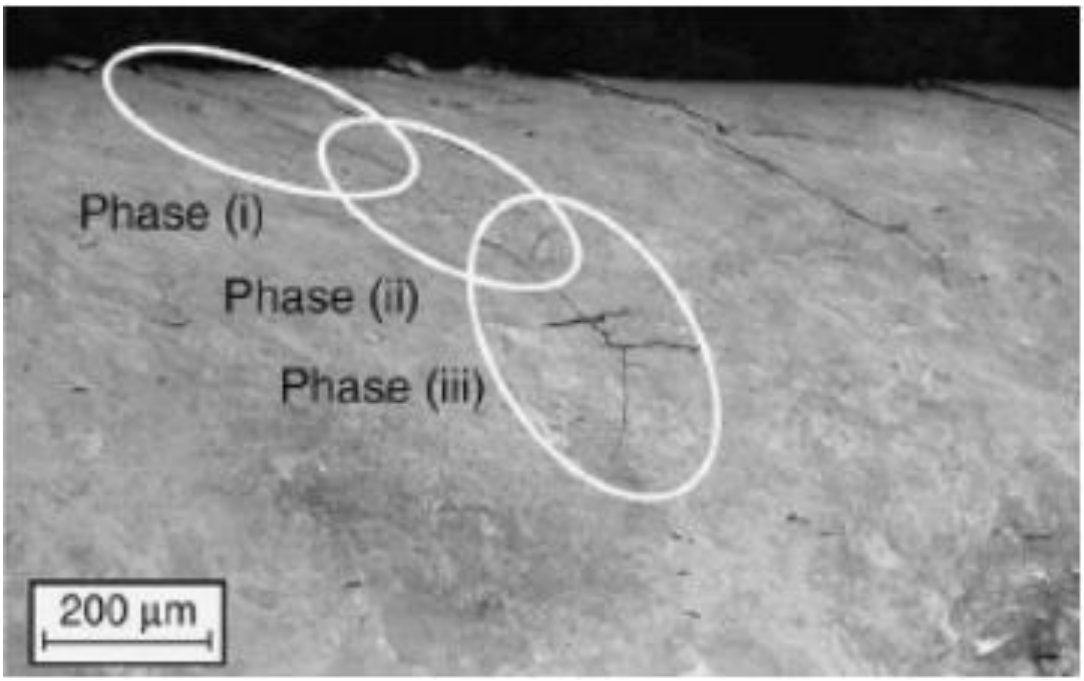

Figure2.10: Three phases of life of a (rolling contact) fatigue crack initiated at the surface of a rail [39].

2.2.2.2 Crack Branching and Deviation

As mentioned, a squat starts growing at a fairly shallow angle relative to the top of the railhead. At a certain length it will either branch/deviate upwards towards the rail surface or branch/deviate downwards. At a crack length of, say, 5 mm branching/deviation upwards will create an uneven rail surface leading to larger contact forces and increased noise and vibration. Downward branching may lead to fracture of the full rail and thereby constitute a risk for derailment [13].

2.2.3 Fracture

Fracture is a form of failure, and is defined as the separation of a solid body into two or more parts under the action of stress. As long as the load is small enough, the structure will only deform elastically. A crack starts to propagate when the crack driving force is larger than the material resistance. If however, the structure is sensitive to cracking due to e.g. inadequate design, defects from manufacturing, handling or bad quality, materials fracture will occur. There are a number of parameters that affect the crack propagation mechanism i.e. material properties, fatigue, loading rate, environment etc [4].

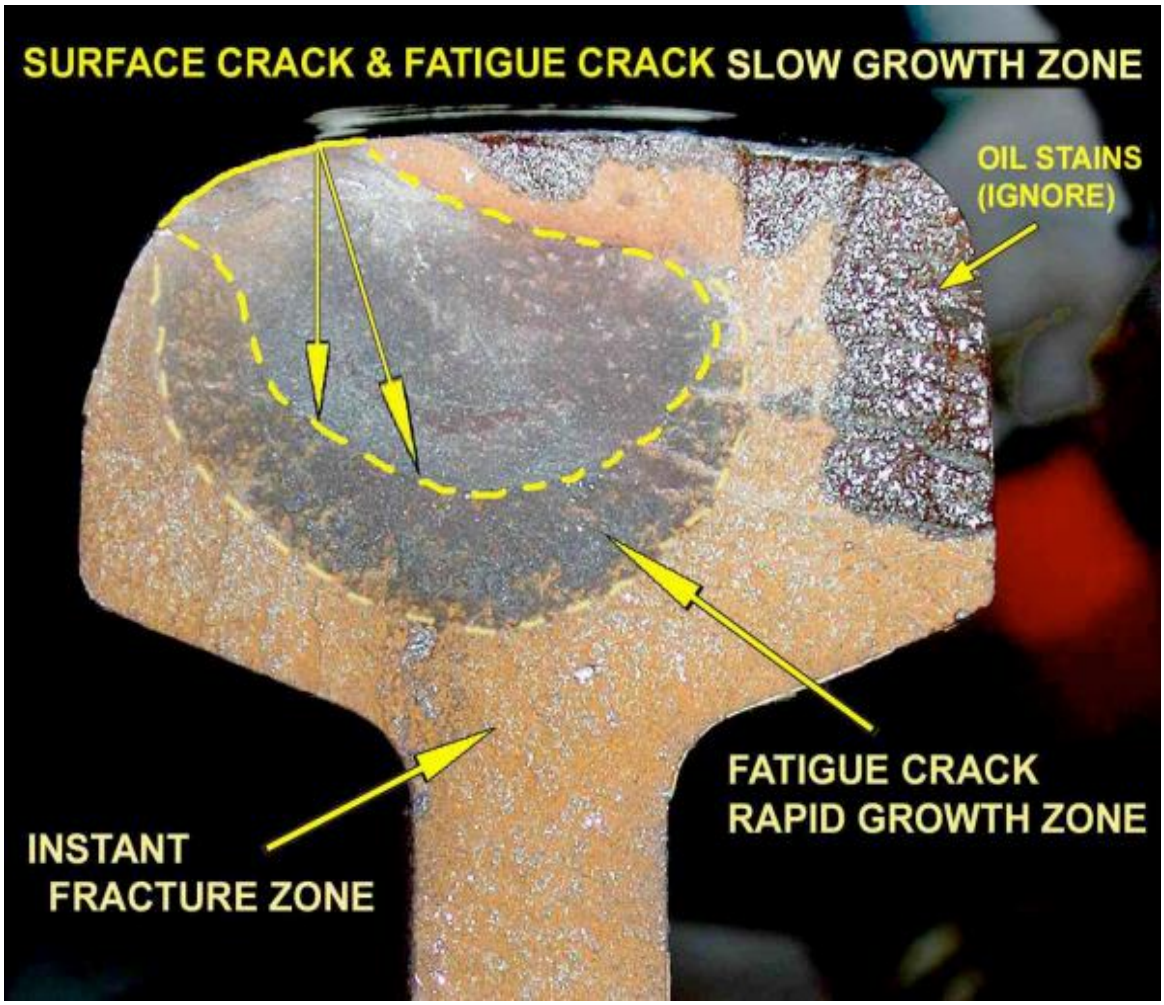

Figure2.11: Complete fracture of rail from a developed RCF crack [4].

Note that RCF crack depth vertically assessed is less than crack depths taken at tangent to surface curvatures containing RCF visual, surface crack. Also note that the crack extends sub-surface toward rail transverse centre. The two growth zones represent the 2nd regime (planar, rippled surface) and the 3rd regime (additional cleavage and micro-void coalescence) of standard fatigue crack growth.

2.3 Review of Related Paper

Elastoplastic computer simulations of the growth of railhead cracks are performed in [14]. Cracks of 3 mm length and larger are studied and competition between wear and crack propagation is considered. The crack growth rate for short cracks is postulated to decrease as their tip moves away from the contact stress field at the rail surface. At a critical length of the crack the growth rate increases since compressive closure forces become lower. It is claimed that the article constitutes the first detailed investigation of the crack driving forces accounting for elastoplastic deformation history.

Surface cracks in rails are discussed in [15]. The conditions of loading, heavy surface plastification and microstructure under which cracks of length 1 mm and larger propagate are described qualitatively and by use of LEFM concepts. The main question is whether a crack will branch into a direction that may cause the entire rail to break. It is suggested that this would only happen if the crack is fairly long and if high tensile stresses induced by low temperatures of the rail would make the mode I stress intensity larger than the mode I threshold value.

In reference [16], the effect of welding residual and thermal stresses on fatigue crack growth in rail welds was studied. The residual stresses in a flash-butt weld were calculated by means of finite element (FE) analysis, and the results were in good agreement with experimentally determined residual stresses in a welded rail. The results from the stabilised stress response in the rail, after several wheel-rail contact load passages, were used to investigate the sensitivity in crack growth in the weld region using fracture mechanics.

Paper [6] study focuses on risk evaluation method for the management to decide a better and cost effective solution that could meet the budgetary constraints regarding renewal, replacement and inspection frequency of rails and wheels. The aim of this paper is to reduce costs and risks related to rail operation by effective decisions related to rail inspection, grinding, lubrications, rectifications and rail replacements. Thus, before development of any model or any empirical relationship associated with risk, familiarity with risk management tools is required.

2.3.1 Gaps on Reviewed Paper

Paper [14] [15] [16] are discussed only on the fatigue life of rail surface crack propagation by using finite element (FE) analysis and linear elastic fracture method. But it is not sufficient to prevent rails from breaking during the service life, In order to prevent rails from breaking during the service life. Ethiopian Railway Corporation has two options in rail defect management. One is to improve the material, making it more durable, the other is to increase the frequency of rail inspection. So this research wills develop Ethiopian Railway Corporation rail inspection and maintenance strategy.

CHAPTER THREE: -RAIL STRESSES ANALYSIS

3.1 Wheel/Rail Material

Surface crack growth resistance of a material depends upon a number of factors, such as its composition, mechanical properties and heat treatment conditions, external loading and the ambient environment. There are two types of steels are generally used for railroad applications: pearlitic and Bainitic steel. Bainitic steel has recently been considered as a candidate material for railroad applications.

For Addis Ababa light rail transit (AALRT), the rail standard used is China National Railways standard of 50 kg/m. Wheel and rail materials are quite similar in composition, differing slightly in the amounts of chemical composition in the steels used. Table1 presents the chemical compositions and shows Main technical parameter of Wheel and rail material [40].

Table 1: The chemical compositions of the AALRT rail material [40]..

Material	C(%)	S(%)	Si(%)	Mn(%)	P(%)	Ni(%)	Cr(%)
Rail	0.8	0.05 max	0.28	1	0.04	-	-

Table 2: Main operational and technical parameter of wheel and rail material [40].

The principal rolling radii of the wheel: R_1^w	420mm
The principal transverse radii of the wheel: R_2^w	∞
The principal rolling radii of the rail: R_1^r	∞
The principal transverse radii of the rail: R_2^r	300mm
Design speed	100Km/h
Yield Stress	540MPa
Ultimate Tensile Strength	780 MPa
Young's Modulus	207 GPa
Poison's Ratio	0.3
Rail Density	7800 kg/m^3
Axle load	250,000 N
Chinese Standard of rail	50 Kg/m
Railway Gauge	1435 mm

3.2 Rail loading and stress

Rails are subjected to primary and secondary loading components. In primary loading, the wheel load is applied from rolling contact to the rail as bending. Stresses arise from the axle static load and the dynamic motions of vehicles (pitch, bounce and rocking) cause fluctuations in the magnitudes of vertical wheel loads on the rail as trains travel over the track. The rail weight itself may also contribute bending stresses. Defects in the running surface of the rails such as joints, dips and twists as well as irregularities in the wheel such as flats and out of roundness may play a role too. Axial stresses arise from structural irregularities of the track and from the acceleration and deceleration of the train during train start and stop.

The forces arising between wheel and rail generate so-called contact stresses in a local volume of the two bodies. The most well-known calculation model is the Hertzian one which will be described in some detail. This model is important since it describes the local stresses with good accuracy for the most common wheel-rail contact problems. Further, it provides a Fracture in rails is a relatively complicated problem. To study fracture, different conditions such as variable and complex loading, secondary stresses, seasonal changes in environmental conditions etc. are taken into account.

3.2.1Hertz Contact Patch Theory

According [18], [19] and [20] the Hertzian contact theory discussed clearly, the contact surface between two curved surfaces, such as a wheel and a rail, can be represented as an ellipse with a major semi-axis a and minor semi-axis b. The pressure exerted over this elliptical area is parabolic in two directions and is defined according to the following equation:

$$P_z(x,y) = p_o\sqrt{1-\frac{x^2}{a^2}-\frac{y^2}{b^2}} \qquad -a \le x \le a \quad and \quad -b \le y \le b \tag{3.1}$$

Where P_0 is the maximum contact pressure at the initial central contact point, and the coordinates x and y refer to distances from the initial contact point along the major semi-axis and minor semi-axis, respectively. The value of P_0 is given by:

$$P_0 = \frac{3}{2}\left(\frac{W}{\pi ab}\right) \tag{3.2}$$

Where: - W is the applied normal force.

Depending on the size and orientation of the contact ellipse the positions of the contact point may be shifted in different directions based on the magnitude of x or y. However, based on the above general Hertz contact formula and assumptions, the stress due to wheel/rail contact decreases and becomes zero if it goes far away from the centreline of the rail head. Similarly, the wheel/rail contact stress is inversely proportional to the major and minor axis of the contact ellipse.

The most important assumptions in Hertz's theory are

- The two contact bodies are linear elastic materials.
- The elastic displacement and the stresses become unnoticeable far from the contact area.
- The radii of the bodies at the contact must be larger than the contact size (semi-infinite bodies are assumed).
- The surfaces are smooth.
- The contact surface is elliptical and the contact pressure distribution is semi-ellipsoid.

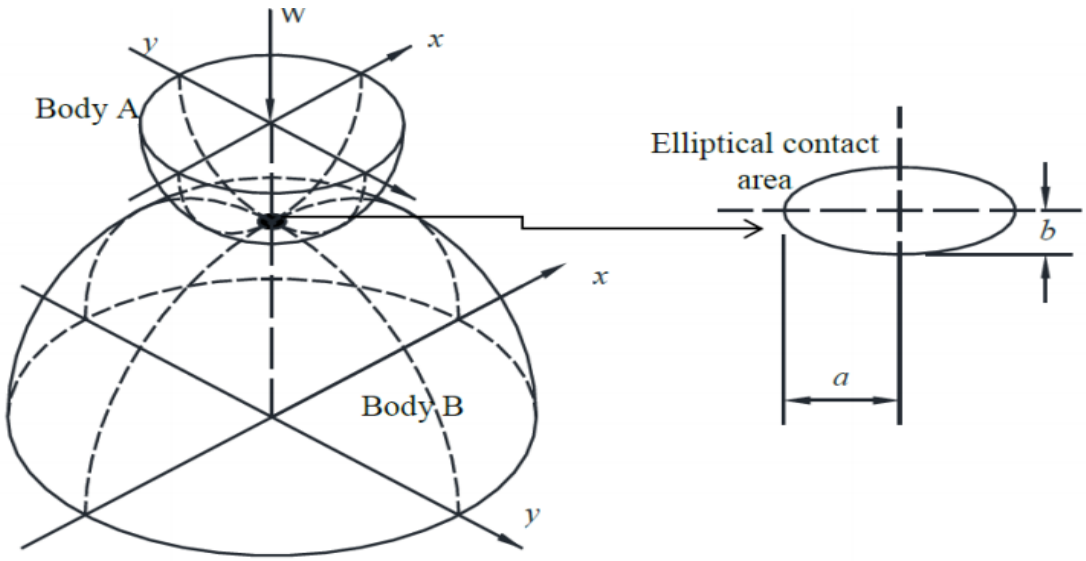

Figure3.1: Geometry of two elastic bodies with convex surfaces in contact [20].

The magnitudes of a and b also depend on the applied normal force, as well as the profile and materials of the wheel and rail. They are expressed as:

$$a = m\left[\frac{3\pi W(K_1+K_2)}{4K_3}\right]^{1/3}, \tag{3.3}$$

$$b = n\left[\frac{3\pi W(K_1+K_2)}{4K_3}\right]^{1/3} \tag{3.4}$$

In the above eguation$K_1, K_2. K_3$ are constants which depend on matrial properties, geometries of the wheel and rail, and are preformed as follows

$$K_1 = \frac{1-(v^w)^2}{\pi E^w} \tag{3.5}$$

$$K_2 = \frac{1-(v^r)^2}{\pi E^r}, \tag{3.6}$$

$$K_3 = \frac{1}{2}\left(\frac{1}{R_1^w} + \frac{1}{R_2^w} + \frac{1}{R_1^r} + \frac{1}{R_2^r}\right), \tag{3.7}$$

Where $E^w and\ v^w$ are young's modulus of the railway wheel material and also $E^w and\ v^w$ are young's modulus of the railway rail material.

The coefficients *m* and *n* in Equations 3.4 and 3.5 are functions of θ.
The variable θ is defined as:

$$\theta = \frac{1}{cos\left(\frac{K_4}{K_3}\right)} \tag{3.8}$$

Where

$$K_4 = \frac{1}{2}\sqrt{\left(\frac{1}{R_1^w} - \frac{1}{R_2^w}\right)^2 + \left(\frac{1}{R_1^r} - \frac{1}{R_2^r}\right)^2 + 2\left(\frac{1}{R_1^w} - \frac{1}{R_2^w}\right)\left(\frac{1}{R_1^r} - \frac{1}{R_2^r}\right)\cos 2\varphi} \tag{3.9}$$

φ (yaw rotation) is the angle of the orientation difference of the principle axes of the two bodies.for the straight segment the cuvature of the rail, $\varphi = 0^0$.

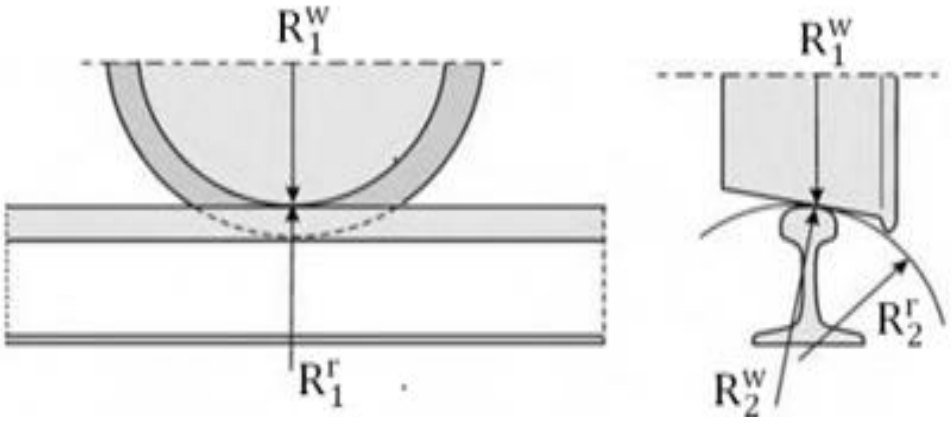

Figure3.2: Wheel rail contact geometry [18].

Case I: - Ifthe principal transverse radii of the rail: $R_2^r = 300$

The principal rolling radii of the wheel: R_1^w=420mm

The principal transverse radii of the wheel: $R_2^w = \infty$

The principal rolling radii of the rail: $R_1^r = \infty$

$$K_1 = \frac{1-(v^w)^2}{\pi E^w} \Rightarrow\Rightarrow K_1 = \frac{1-(0.3^w)^2}{\pi \times 207 \times 10^9\, N/m^2} \Rightarrow\Rightarrow \boldsymbol{K_1 = 1.456 \times 10^{-12}\, m^2/N}$$

$$K_1 = \frac{1-(v^r)^2}{\pi E^r} \Rightarrow\Rightarrow K_2 = \frac{1-(0.3^w)^2}{\pi \times 207 \times 10^9\, N/m^2} \Rightarrow\Rightarrow \boldsymbol{K_2 = 1.456 \times 10^{-12}\, m^2/N}$$

$$K_3 = \frac{1}{2}\left(\frac{1}{R_1^w} + \frac{1}{R_2^w} + \frac{1}{R_1^r} + \frac{1}{R_2^r}\right) \Rightarrow\Rightarrow K_3 = \frac{1}{2}\left(\frac{1}{420} + \frac{1}{\infty} + \frac{1}{300} + \frac{1}{\infty}\right) \Rightarrow\Rightarrow \boldsymbol{K_3 = 0.00286/mm}$$

The hertz coefficients m and n are function of the angular parameter θ which is given by

$$\theta = \frac{1}{cos\left(\frac{K_4}{K_3}\right)} \tag{3.10}$$

Then eqn.3.9 $K_4 = \frac{1}{2}\sqrt{\left(\frac{1}{R_1^w} - \frac{1}{R_2^w}\right)^2 + \left(\frac{1}{R_1^r} - \frac{1}{R_2^r}\right)^2 + 2\left(\frac{1}{R_1^w} - \frac{1}{R_2^w}\right)\left(\frac{1}{R_1^r} - \frac{1}{R_2^r}\right)\cos 2\varphi}$

φ (yaw rotation) is the angle of the orientation difference of the principle axes of the two bodies.for the straight segment the cuvature of the rail, $\varphi = 0^0$.

$$K_4 = \frac{1}{2}\sqrt{\left(\frac{1}{420} - \frac{1}{\infty}\right)^2 + \left(\frac{1}{\infty} - \frac{1}{300}\right)^2 + 2\left(\frac{1}{420} - \frac{1}{\infty}\right)\left(\frac{1}{\infty} - \frac{1}{300}\right)\cos 2(0^0)}$$

$$\boldsymbol{K_4 = 4.76 * e^{-4}/mm}$$

Therfore from eqn 3.10 a straight rail segment,θ is defined as:

$$\theta = \frac{1}{cos\left(\frac{K_4}{K_3}\right)}$$

$$\theta = \frac{1}{cos\left(\frac{4.76*e^{-4}}{0.00286}\right)}$$

$$\boldsymbol{\theta = 80.4^0}$$

Table 3: Hertz coefficients m and n [41]

$\theta(deg)$	M	N	$\theta(deg)$	M	N
0.5	61.4	0.1018	40	2.136	0.567
1	36.89	0.1314	45	1.926	0.604
1.5	27.48	0.1522	50	1.754	0.641
2	22.26	0.1691	55	1.611	0.678
3	16.5	0.1964	60	1.4186	0.717
4	13.31	0.2188	65	1.378	0.759
6	9.79	0.2552	70	1.284	0.802
8	7.86	0.285	75	1.202	0.846
10	6.604	0.3112	80	1.128	0.893
20	3.813	0.4125	85	1.061	0.944
30	2.731	0.493	90	1.0	1.0
35	2.397	0.530			

From the above table the value of m and n can be calculated by interpolation method

$$\theta_1 = 80^0, \quad m_1 = 1.128\,,\ n_1 = 0.893, \quad \theta_2 = 85^0,\ m_2 = 1.061,\ n_2 = 0.944$$

$$m = m_1 + \frac{m_2 - m_1}{\theta_2 - \theta_1}(\theta - \theta_1)$$

$$m = 1.128 + \frac{1.061 - 1.128}{85 - 80}(80.4 - 80)$$

$$\boldsymbol{m = 1.123}$$

Also, $$n = n_1 + \frac{n_2 - n_1}{\theta_2 - \theta_1}(\theta - \theta_1)$$

$$n = 0.893 + \frac{0.944 - 0.893}{85 - 80}(80.4 - 80)$$

$$\boldsymbol{n = 0.897}$$

The forces imposed on the track structure could be classified as mechanical (both static and dynamic) and thermal. Paper [22] discussed the type of forces and their source as: (a) quasi-static loads induced by the self-weight of the vehicle and reaction forces in curves; (b)

dynamic loads resulting from track irregularities; and (c) thermal loading due to temperature variations in continuous welded rail (CWR).

Vertical forces are perpendicular to the plane of the rails and may be vertical wheel load or uplift force (reaction to wheel load) and are those forces result the mechanical stresses in the track [23]. The general method used in the determination of the design vertical wheel load according to Doyle (1980) is to empirically express it as a function of the static wheel load, i.e.

$$W = \emptyset\, w_s \tag{3.11}$$

Where: W=design wheel load (KN),

w_s = static wheel load (KN), and

$\emptyset$ = dimensionless impact factor (always >l).

The nominal vehicle axle load is usually measured for the static condition, but in the design of railway track the actual stresses in the various components of the track structure and in the rolling stock must be determined from the dynamic vertical and lateral forces imposed by the design vehicle moving at designed speed. Dynamic impact factor is a corrective factor to compensate for dynamic as well as impact effects of wheel load resulted from wheel and rail surface irregularities [24].

Table 4: Recommended relationship for dynamic coefficient factors [25]

Recommender	Formula
AREMA	$\emptyset = 1 + 5.21\frac{V}{D}$
DB	$\emptyset = 1 + \frac{V^2}{3*10^4}$ for V≤100 km/hr $\emptyset = 1 + \frac{4.5*V^2}{10^5} - \frac{1.5*V^3}{10^7}$, for V > 100km/hr
India	$\emptyset = 1 + \frac{V}{58.14k^{0.5}}$
South Africa	$\emptyset = 1 + 4.92\frac{V}{D}$ for narrow gage

Where: V= Vehicle speed (Km/hr); D= wheel diameter (mm); and k = track modulus (Mpa)

The axial load was chosen as 250KN.The load for each wheel was then taken to be 125KN. To determine the vertical wheel load on the rail, the dynamic impact factor expression recommended by AREMA was used and the vehicle speed for national railway network of Ethiopia was taken as 80Km/hr and the wheel diameter as 0.84m. So, the standard vertical wheel load for AALRT is taken as **W= 187,023.8N.**

By using eqn 3.3 and 3.4 the vaue of a and b will be;

$$a = m\left[\frac{3\pi W(K_1 + K_2)}{4K_3}\right]^{1/3}$$

$$a = 1.0324\left[3 \times \pi \times 187{,}023\frac{\left(2 \times 1.456 \times 10^{-12}\frac{m^2}{N}\right)}{4 \times 2.86/m}\right]^{\frac{1}{3}}$$

$$\boldsymbol{a = 0.0086m}$$

$$b = n\left[\frac{3\pi W(K_1 + K_2)}{4K_3}\right]^{1/3}$$

$$b = 0.9676\left[\frac{3 \times \pi \times 187{,}023\left(2 \times 1.456 \times 10^{-12}\frac{m^2}{N}\right)}{4 \times 2.86/m}\right]^{1/3}$$

$$\boldsymbol{b = 0.00687m}$$

The maximum Hertz contact stress on the centre of rail head the contact pressure (stress) is equal to:

$$P_O = \frac{3W}{2\pi ab} \tag{3.11}$$

$$P_O = \frac{3 \times 187{,}023}{2 \times \pi \times 0.0086 \times 0.00687}$$

$$\boldsymbol{P_O = 1511.22MPa}$$

To determine the size of the contact area, determination of the orientation of the shape of the contact ellipse is necessary.

$$\frac{1}{R_1^w}+\frac{1}{R_1^r}\geq\frac{1}{R_2^w}+\frac{1}{R_2^r}$$

$$\frac{1}{420}+\frac{1}{\infty}\leq\frac{1}{\infty}+\frac{1}{300}$$

Therefore, the transverse semi axis of the contact ellipse (y direction) is less than or equal to the longitudinal semi-axis. The contact ellipse major axis a, is along the length of the rail and the contact ellipse minor axis b is along the width of the rail.

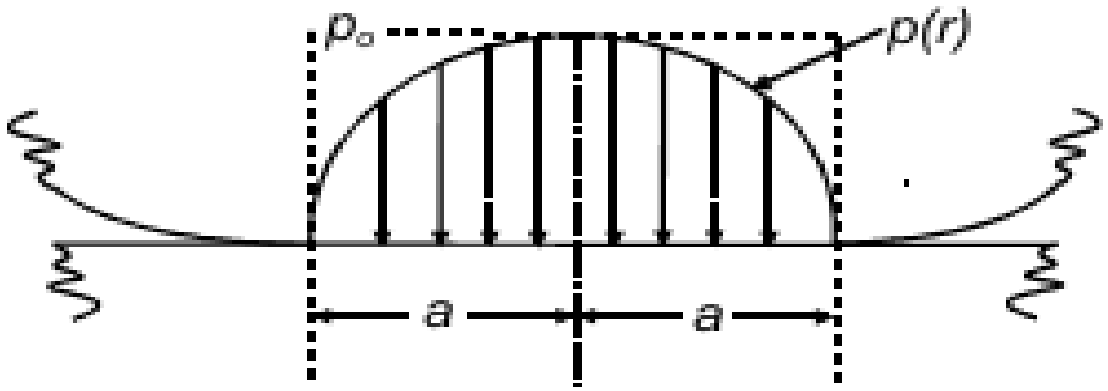

Figure3.3: wheel rail contact pressure distribution [18]

The result contact area was an ellipse with a contact patch area of π*a*b=187.7mm^2.The equation for the resulting pressure distribution is

$$P_z(x,y)=1511.22\ MPa\sqrt{1-\left(\frac{x}{0.0087m}\right)^2-\left(\frac{y}{0.00687m}\right)^2} \tag{3.12}$$

This parabolic distribution was applied to the finite element model, approximated as multiple uniform pressures over small areas. The angular velocity of the wheel with maximum operating speed of the vehicle is

$$\omega=\frac{v}{R_1^w} \tag{3.13}$$

Where v is the maximum operation speed of the vehicle, 100km/hr = 27.77m/s and

R_1^w is the principal rolling radius of the wheel, 420mm = 0.42m.

$$\omega=\frac{27.77}{0.42}=66.12\ \text{rad/s}$$

Case II: - If the principal transverse radii of the rail: $R_2^r = 295$

The principal rolling radii of the wheel: R_1^w=420mm

The principal transverse radii of the wheel: $R_2^w = \infty$

The principal rolling radii of the rail: $R_1^r = \infty$

$$K_1 = \frac{1-(v^w)^2}{\pi E^w} \Rightarrow\Rightarrow K_1 = \frac{1-(0.3^w)^2}{\pi \times 207 \times 10^9\, N/m^2} \Rightarrow\Rightarrow \boldsymbol{K_1 = 1.456 \times 10^{-12}\, m^2/N}$$

$$K_1 = \frac{1-(v^r)^2}{\pi E^r} \Rightarrow\Rightarrow K_2 = \frac{1-(0.3^w)^2}{\pi \times 207 \times 10^9\, N/m^2} \Rightarrow\Rightarrow \boldsymbol{K_2 = 1.456 \times 10^{-12}\, m^2/N}$$

$$K_3 = \frac{1}{2}\left(\frac{1}{R_1^w} + \frac{1}{R_2^w} + \frac{1}{R_1^r} + \frac{1}{R_2^r}\right) \Rightarrow\Rightarrow K_3 = \frac{1}{2}\left(\frac{1}{420} + \frac{1}{\infty} + \frac{1}{295} + \frac{1}{\infty}\right) \Rightarrow\Rightarrow \boldsymbol{K_3 = 0.002885/mm}$$

The hertz coefficients m and n are function of the angular parameter θ which is given by

Then eqn.3.9

$$K_4 = \frac{1}{2}\sqrt{\left(\frac{1}{R_1^w} - \frac{1}{R_2^w}\right)^2 + \left(\frac{1}{R_1^r} - \frac{1}{R_2^r}\right)^2 + 2\left(\frac{1}{R_1^w} - \frac{1}{R_2^w}\right)\left(\frac{1}{R_1^r} - \frac{1}{R_2^r}\right)\cos 2\varphi}$$

φ (yaw rotation) is the angle of the orientation difference of the principle axes of the two bodies.for the straight segment the cuvature of the rail, $\varphi = 0^0$.

$$K_4 = \frac{1}{2}\sqrt{\left(\frac{1}{420} - \frac{1}{\infty}\right)^2 + \left(\frac{1}{\infty} - \frac{1}{295}\right)^2 + 2\left(\frac{1}{420} - \frac{1}{\infty}\right)\left(\frac{1}{\infty} - \frac{1}{295}\right)\cos 2(0^0)}$$

$$\boldsymbol{K_4 = 5.019 * e^{-4}/mm}$$

Therfore from eqn 3.10 a straight rail segment,θ is defined as:

$$\theta = \frac{1}{cos\left(\frac{K_4}{K_3}\right)}$$

$$\theta = \frac{1}{cos\left(\frac{\mathbf{5.019 * e^{-4}}}{\mathbf{0.002885}}\right)}$$

$$\boldsymbol{\theta = 79.97^0}$$

From table 3 the value of m and n can be calculated by interpolation method

$$\theta_1 = 75^0, \quad m_1 = 1.202\,, n_1 = 0.846, \quad \theta_2 = 80^0, \quad m_2 = 1.128, \quad n_2 = 0.893$$

$$m = m_1 + \frac{m_2 - m_1}{\theta_2 - \theta_1}(\theta - \theta_1) \Rightarrow\gg m = 1.202 + \frac{1.128 - 1.202}{80 - 75}(79.97 - 75)$$

$$\boldsymbol{m = 1.129}$$

Also, $n = n_1 + \frac{n_2 - n_1}{\theta_2 - \theta_1}(\theta - \theta_1) \Rightarrow\gg n = 0.846 + \frac{0.893 - 0.846}{80 - 75}(79.97 - 75)$

$$\boldsymbol{n = 0.8927}$$

Then the value of a and b can be calcualte as

$$a = m\left[\frac{3\pi W(K_1 + K_2)}{4K_3}\right]^{1/3}$$

$$a = 1.129\left[3 \times \pi \times 187{,}023\frac{\left(2 \times 1.456 \times 10^{-12}\frac{m^2}{N}\right)}{4 \times 2.885/m}\right]^{\frac{1}{3}}$$

$$\boldsymbol{a = 0.008618m}$$

$$b = n\left[\frac{3\pi W(K_1 + K_2)}{4K_3}\right]^{1/3}$$

$$b = 0.8927\left[\frac{3 \times \pi \times 187{,}023\left(2 \times 1.456 \times 10^{-12}\frac{m^2}{N}\right)}{4 \times 2.885/m}\right]^{1/3}$$

$$\boldsymbol{b = 0.0068143m}$$

The maximum Hertz contact stress on the centre of rail head the contact pressure (stress) is equal to:

$$P_O = \frac{3W}{2\pi ab} \Rightarrow\gg P_O = \frac{3 \times 187{,}023}{2 \times \pi \times 0.008618 \times 0.0068143}$$

$$\boldsymbol{P_O = 1520.577MPa}$$

Case III: - If the principal transverse radii of the rail: $R_2^r = 290$

The principal rolling radii of the wheel: R_1^w=420mm

The principal transverse radii of the wheel: $R_2^w = \infty$

The principal rolling radii of the rail: $R_1^r = \infty$

$$K_1 = \frac{1-(v^w)^2}{\pi E^w} \Rightarrow\Rightarrow K_1 = \frac{1-(0.3^w)^2}{\pi \times 207 \times 10^9\, N/m^2} \Rightarrow\Rightarrow \boldsymbol{K_1 = 1.456 \times 10^{-12}\, m^2/N}$$

$$K_1 = \frac{1-(v^r)^2}{\pi E^r} \Rightarrow\Rightarrow K_2 = \frac{1-(0.3^w)^2}{\pi \times 207 \times 10^9\, N/m^2} \Rightarrow\Rightarrow \boldsymbol{K_2 = 1.456 \times 10^{-12}\, m^2/N}$$

$$K_3 = \frac{1}{2}\left(\frac{1}{R_1^w} + \frac{1}{R_2^w} + \frac{1}{R_1^r} + \frac{1}{R_2^r}\right) \Rightarrow\Rightarrow K_3 = \frac{1}{2}\left(\frac{1}{420} + \frac{1}{\infty} + \frac{1}{290} + \frac{1}{\infty}\right) \Rightarrow\Rightarrow \boldsymbol{K_3 = 0.002914/mm}$$

The hertz coefficients m and n are function of the angular parameter θ which is given by

Then eqn.3.9

$$K_4 = \frac{1}{2}\sqrt{\left(\frac{1}{R_1^w} - \frac{1}{R_2^w}\right)^2 + \left(\frac{1}{R_1^r} - \frac{1}{R_2^r}\right)^2 + 2\left(\frac{1}{R_1^w} - \frac{1}{R_2^w}\right)\left(\frac{1}{R_1^r} - \frac{1}{R_2^r}\right)\cos 2\varphi}$$

φ (yaw rotation) is the angle of the orientation difference of the principle axes of the two bodies.for the straight segment the cuvature of the rail, $\varphi = 0^0$.

$$K_4 = \frac{1}{2}\sqrt{\left(\frac{1}{420} - \frac{1}{\infty}\right)^2 + \left(\frac{1}{\infty} - \frac{1}{290}\right)^2 + 2\left(\frac{1}{420} - \frac{1}{\infty}\right)\left(\frac{1}{\infty} - \frac{1}{290}\right)\cos 2(0^0)}$$

$$\boldsymbol{K_4 = 5.3366 * e^{-4}/mm}$$

Therfore from eqn 3.10 a straight rail segment,θ is defined as:

$$\theta = \frac{1}{cos\left(\frac{K_4}{K_3}\right)}$$

$$\theta = \frac{1}{cos\left(\frac{\mathbf{5.3366 * e^{-4}}}{\mathbf{0.002914}}\right)}$$

$$\boldsymbol{\theta = 79.44^0}$$

From table 3 the value of m and n can be calculated by interpolation method

$$\theta_1 = 75^0, \quad m_1 = 1.202\,, n_1 = 0.846, \quad \theta_2 = 80^0, \quad m_2 = 1.128, \quad n_2 = 0.893$$

$$m = m_1 + \frac{m_2 - m_1}{\theta_2 - \theta_1}(\theta - \theta_1) \Rightarrow\gg m = 1.202 + \frac{1.128 - 1.202}{80 - 75}(79.44 - 75)$$

$$\boldsymbol{m = 1.136}$$

Also, $n = n_1 + \frac{n_2 - n_1}{\theta_2 - \theta_1}(\theta - \theta_1) \Rightarrow\gg n = 0.846 + \frac{0.893 - 0.846}{80 - 75}(79.44 - 75)$

$$\boldsymbol{n = 0.8877}$$

Then the value of a and b can be calcualte as

$$a = m\left[\frac{3\pi W(K_1 + K_2)}{4K_3}\right]^{1/3}$$

$$a = 1.136\left[3 \times \pi \times 187{,}023\frac{\left(2 \times 1.456 \times 10^{-12}\frac{m^2}{N}\right)}{4 \times 2.914/m}\right]^{\frac{1}{3}}$$

$$\boldsymbol{a = 0.008642m}$$

$$b = n\left[\frac{3\pi W(K_1 + K_2)}{4K_3}\right]^{1/3}$$

$$b = 0.8877\left[\frac{3 \times \pi \times 187{,}023\left(2 \times 1.456 \times 10^{-12}\frac{m^2}{N}\right)}{4 \times 2.914/m}\right]^{1/3}$$

$$\boldsymbol{b = 0.006753m}$$

The maximum Hertz contact stress on the centre of rail head the contact pressure (stress) is equal to:

$$P_O = \frac{3W}{2\pi ab} \Rightarrow\gg P_O = \frac{3 \times 187{,}023}{2 \times \pi \times 0.008642 \times 0.006753}$$

$$\boldsymbol{P_O = 1530.119MPa}$$

3.3 Finite Element method Analysis

3.3.1 Finite Element Method Analysis for Case I:

3.3.1.1 Finite Element model

In order to build a realistic model of wheel/rail contact problem a 3D elasto-plastic finite element model is needed. This model should be able to accurately calculate the 3D stress response in the contact region as well as includes both material and geometric nonlinearity. To model the principal transverse radii of the rail is $300mm$for national railway network of Ethiopia for the purpose of analysing the rail stresses. For the analysis implementation, the three dimensional rail of T-50 profile with 0.6m length was modelled. The cause for choosing such a length was that the two sleepers could be placed underneath the rail at the standard distances of 0.6m. The model is constructed by SOLIDWORK software and imported to ANSYS 14.2 workbench.

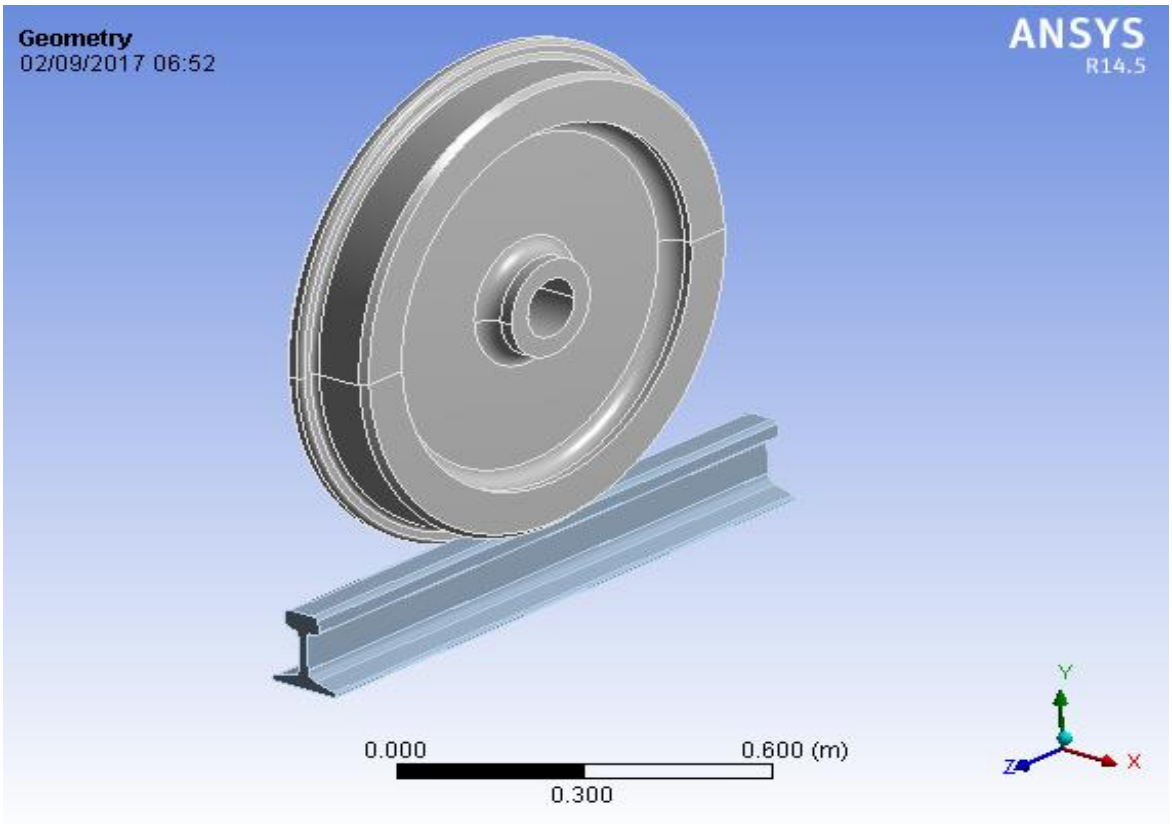

Figure3.4: Geometric model of wheel and rail

3.3.1.2 wheel-rail Meshing

For this fatigue life analysis test, we are going to use one side wheel and rail model. After giving the connection bond between wheel and rail, meshing of both parts follow.

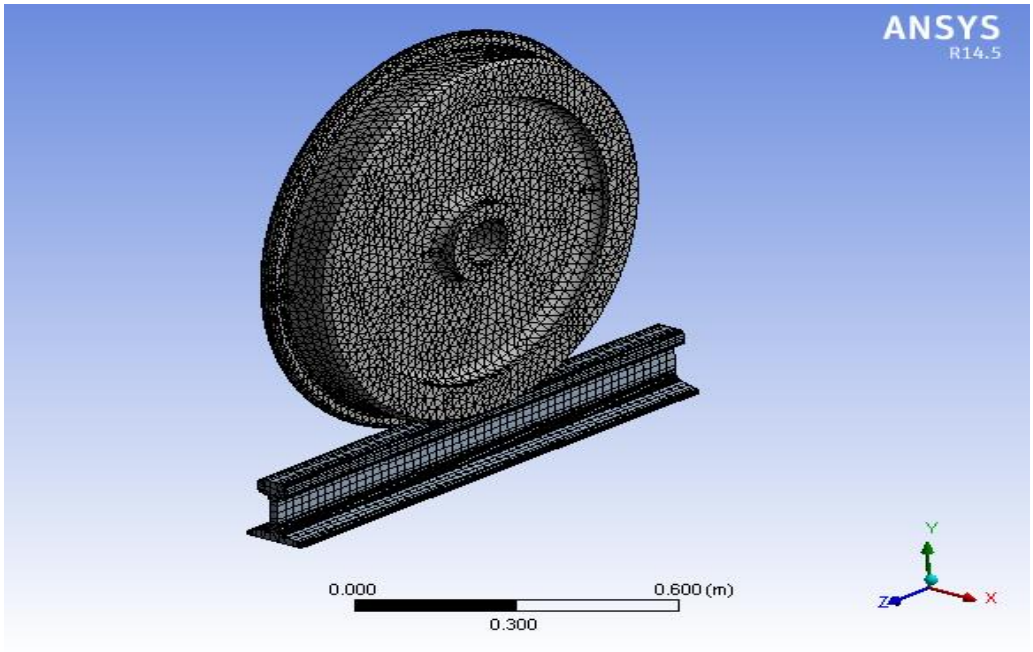

Figure3.5: wheel-rail meshing created by ANSYS 14.5for Case I

The wheel/rail model considered in this thesis consists of 39648 numbers of elements and 93357 numbers of nodes. The mesh size consideration is limited with analysis time and result accuracy. The mesh size considered for the wheel/rail was finer.

3.3.1.3 Loading and Boundary Conditions

Fixed boundary condition is applied to the rail at the bottom of the foot. Force is applied on the wheel and the rotational velocity of the wheel is applied to the wheel centre. Also the standard earth gravity is applied. All model components are only allowed to move (displace) vertically i.e. in y-axis, so the model is restrained on left and right side because of continuity.

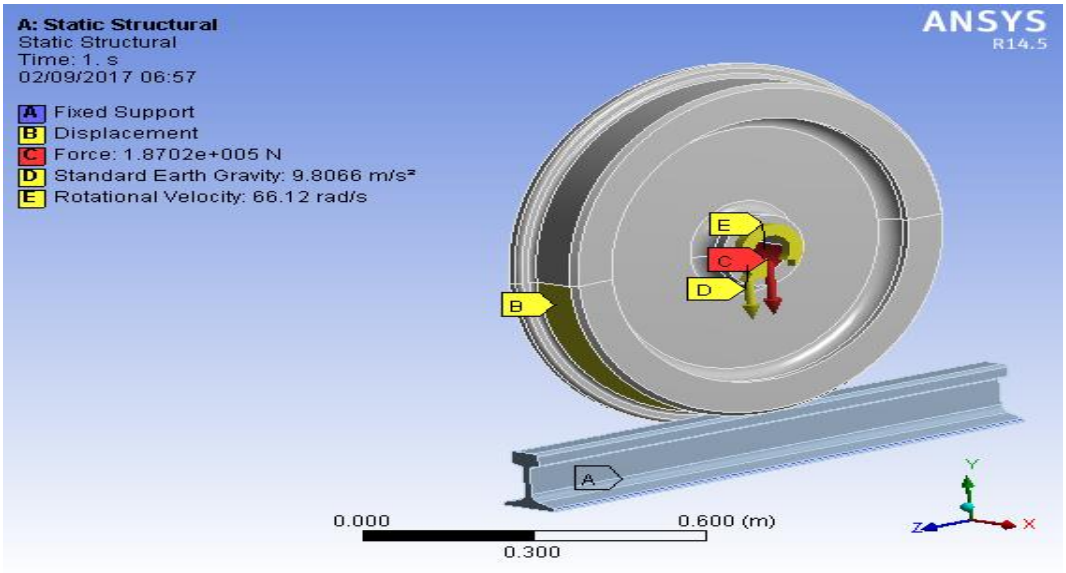

Figure3.6: Wheel/Rail boundary conditions and input data for Case I

3.3.1.4 Simulation Results

After performing the simulation in ANSYS 14.5 the results are obtained in the form of stress distributions. The results obtained from ANSYS 14.5 are described as follows;

3.3.1.4.1 Stress distribution results

Therefore, from the stress distribution results obtained in the form of Von-Misses stresses and the maximum value is found to be 133.85MPa.

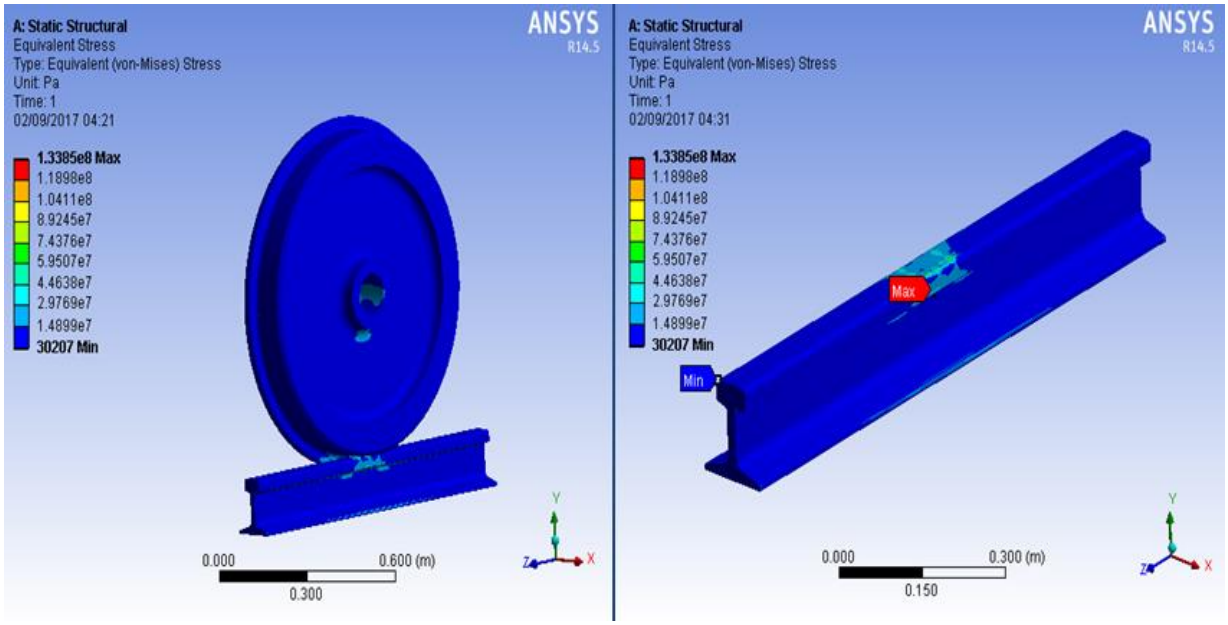

Figure3.7: Contour plot of Equivalent (von-mises) stress for Case I

3.3.1.4.2 Equivalent elastic strain

As shown figures below, the maximum and minimum values of equivalent elastic strain on the rail is (0.00076maximum and 1.46×10^{-7}minimum values).

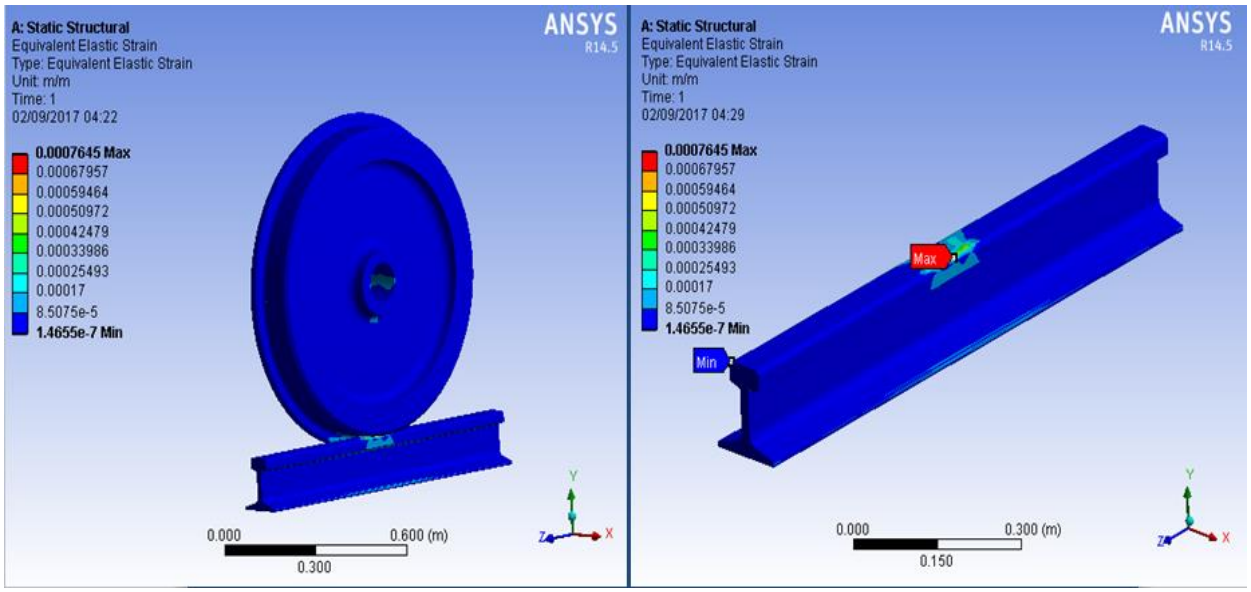

Figure3.8: Contour plot of Equivalent elastic strain for Case I

3.3.1.4.3 Total deformation

As shown figures below, the maximum values of Total deformation on the wheel/rail is 3.211×10^{-5}m.

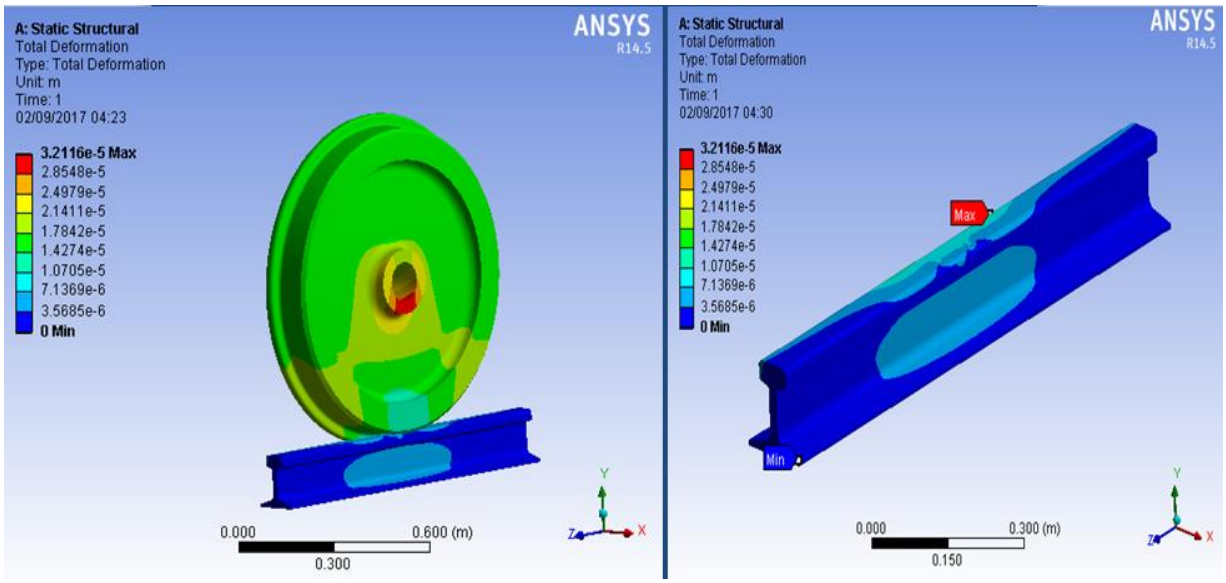

Figure3.9: Contour plot of Total deformation for Case I

3.3.2 Finite Element Method Analysis for Case II:

3.3.2.1 Simulation Results

The principal transverse radius of 295mm T50 rail model for the FEA is created. After performing the simulation in ANSYS 14.5 the results are obtained in the form of stress distributions. The results obtained from ANSYS 14.5 are described as follows;

3.3.2.1.1 Stress distribution results

Therefore, from the stress distribution results obtained in the form of Von-Misses stresses and the maximum value is found to be 168.72MPa.

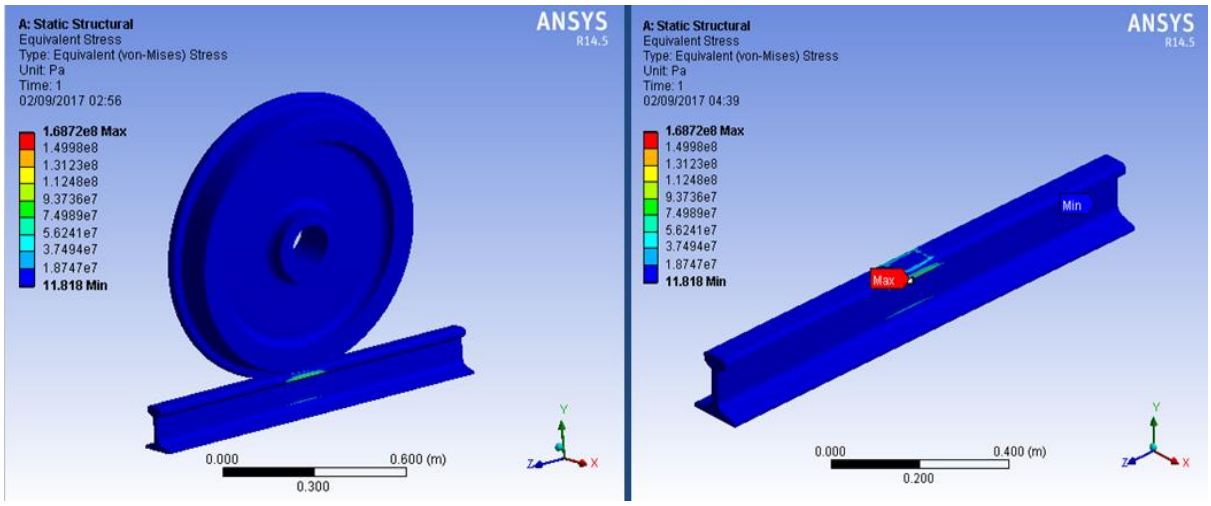

Figure3.10: Contour plot of Equivalent (von-mises) stress for Case II

3.3.2.1.2 Equivalent elastic strain

As shown figures below, the maximum and minimum values of equivalent elastic strain on the rail is (0.000877maximum and 3.04×10^{-10}minimum values).

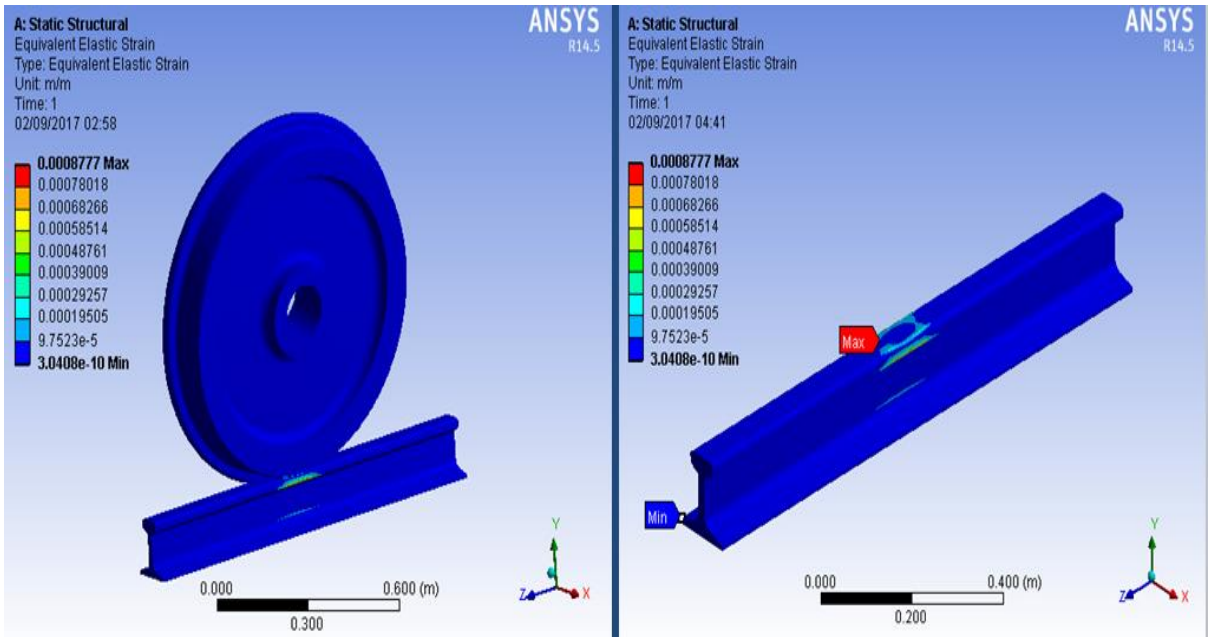

Figure3.11: Contour plot of Equivalent elastic strain for Case II

3.3.2.1.3 Total deformation

As shown figures below, the maximum values of Total deformation on the wheel/rail is 3.461×10^{-5}m.

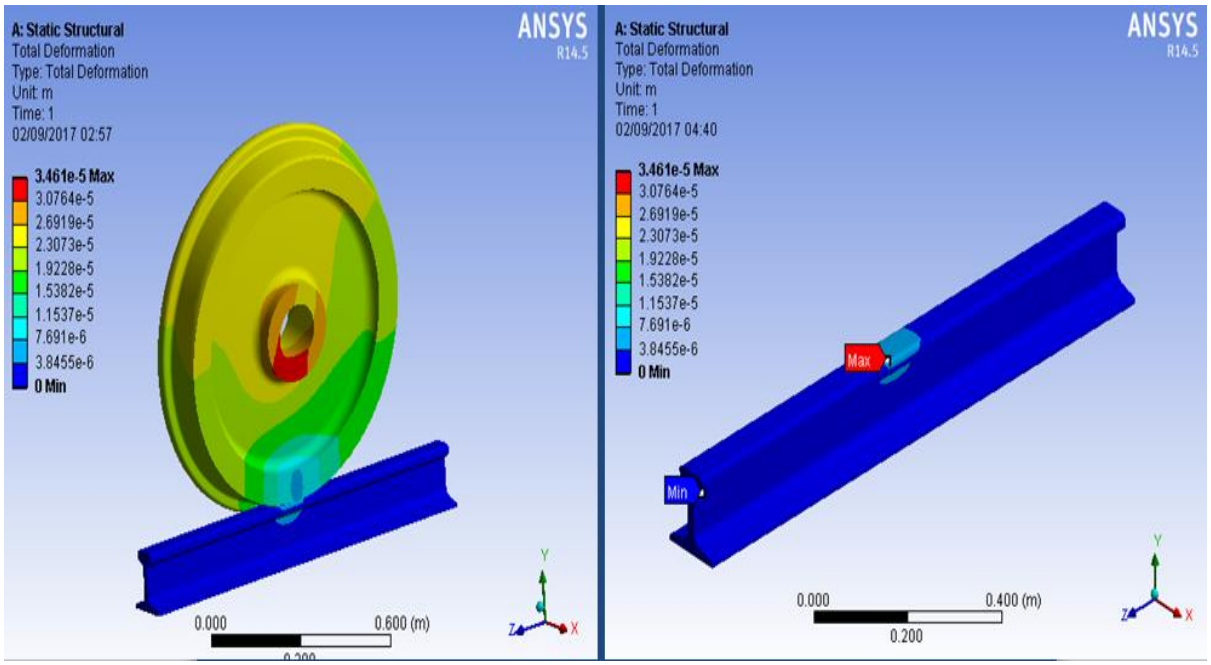

Figure3.12: Contour plot of Total deformation for Case II

3.3.3Finite Element Method Analysis for Case III:

3.3.3.1 Simulation Results

The principal transverse radius of 290mm T50 rail model for the FEA is created. After performing the simulation in ANSYS 14.5 the results are obtained in the form of stress distributions. The results obtained from ANSYS 14.5 are described as follows;

3.3.3.1.1 Stress distribution results

Therefore, from the stress distribution results obtained in the form of Von-Misses stresses and the maximum value is found to be 178.62MPa. I.e. the equivalent alternating stress is increases as the load increases.

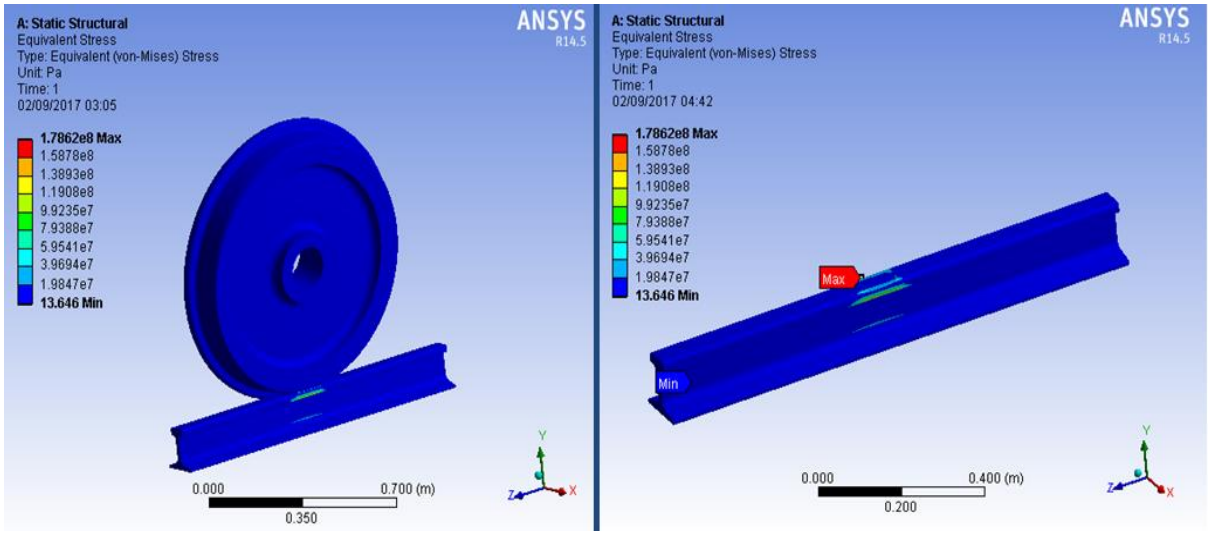

Figure3.13: Contour plot of Equivalent (von-mises) stress for Case III

3.3.3.1.2 Equivalent elastic strain

As shown figures below, the maximum and minimum values of equivalent elastic strain on the rail is (0.000884maximum and 3.04×10^{-10}minimum values).

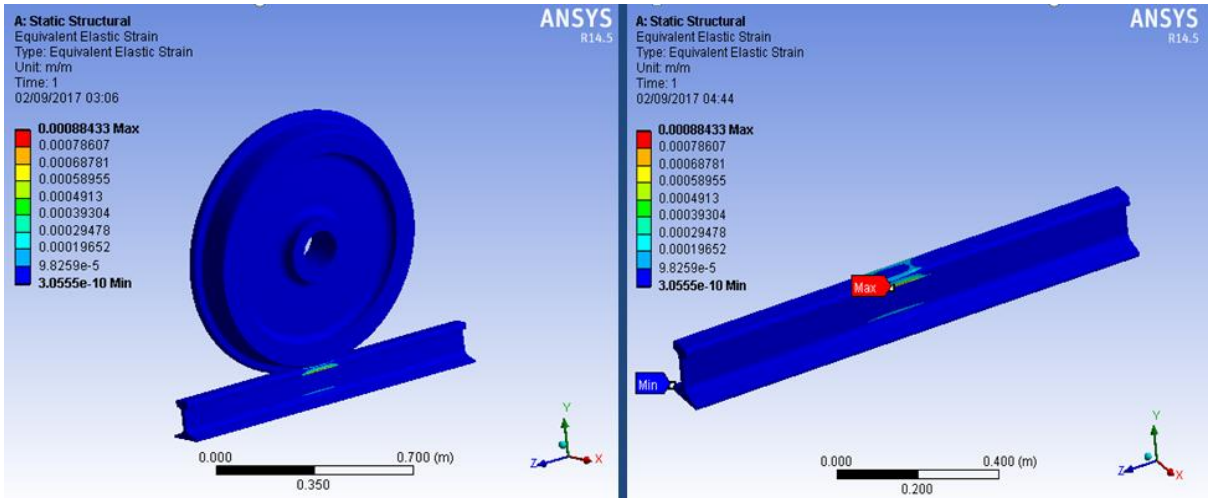

Figure3.14: Contour plot of Equivalent elastic strain for Case III

3.3.3.1.3 Total deformation

As shown figures below, the maximum values of Total deformation on the wheel/rail is 3.4336×10^{-5}m.

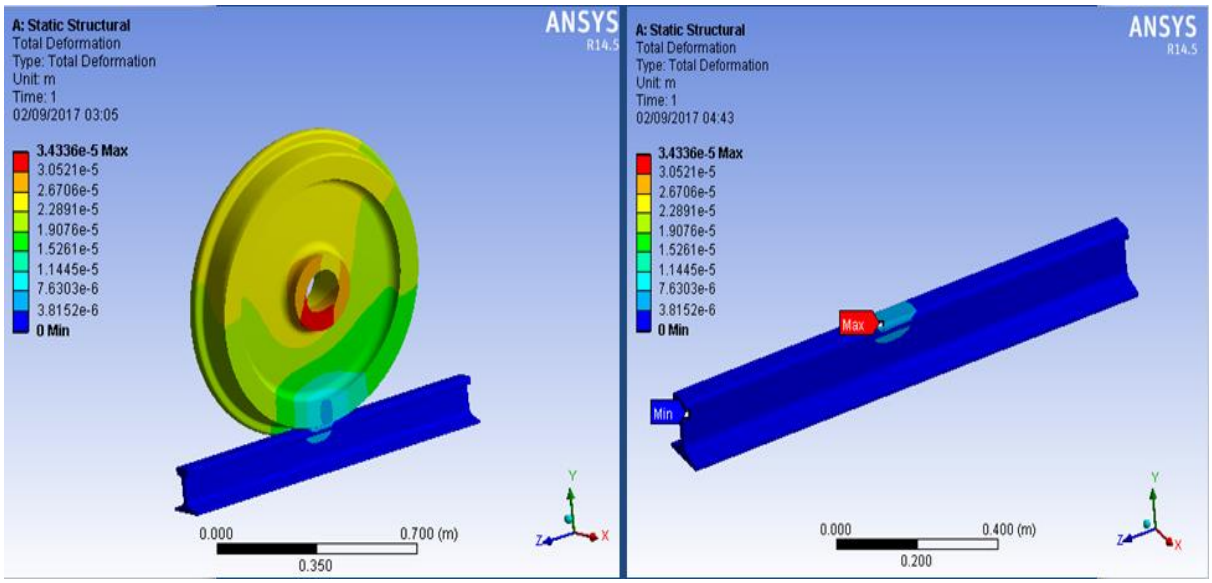

Figure3.15: Contour plot of Total deformation for Case III

CHAPTER FOUR: - LINEAR ELASTIC FRACTURE MECHANICS ANALYSIS

4.1 Introduction

Linear-elastic fracture mechanics (LEFM) method will develop the skills for a mathematical background in determining the elastic stress field equations around a crack tip. The field equations are assumed to be within a small plastic zone ahead of the crack tip. If this plastic zone is sufficiently small, the small-scale yielding approach is used for characterizing brittle solids and for determining the stress and strain fields when the size of the plastic zone is sufficiently smaller than the crack length. Assuming the geometry has very small displacement and the material is elastic, homogeneous and isotropic. Linear Elastic Fracture Mechanics (LEFM) principles are used to relate the stress magnitude and distribution near the crack tip to the remote stresses applied to the cracked component, crack size, crack shape and the material properties of the cracked component [26]. The general form of the LEFM equation is given as:

$$\sigma_{ij} = \frac{K_{II}}{\sqrt{2\pi r}} f_{ij}(\theta) + \cdots \tag{4.1}$$

Where

K_{II} =Mode II stress intensity factor

r =distance from the crack tip

$f_{ij}(\theta)$ = function that represent the stress dependence onθ.

The general form of the LEFM equations is given in equation (4.1). As seen, a singularity exists such as r, the distance from the crack tip, tends toward zero, the stresses go to infinity. As the yield stress is exceeded, material deforms plastically and a plastic zone is formed near the crack tip. The basis of LEFM remains valid if this region of plasticity remains small in relation to the overall dimensions of the crack and cracked body.

The application of Linear Elastic Fracture Mechanics to surface defects requires the knowledge of stress intensity factor. The stress intensity factor, K is used in fracture mechanics to predict the stress state (stress intensity) near the tip of a crack caused by a remote load or residual stresses. The magnitude of K depends on sample geometry, the size and location of the crack, and the magnitude and the modal distribution of load on the material.

4.1.1Modes of Loading

A crack in a body may be subjected to three different types of loading, which involve displacements of the crack surfaces.

Mode I: Opening or tensile mode (corresponds to fracture where the crack surfaces are displaced normal to themselves. This is a typical tensile type of fracture)

Mode II: Sliding or in-plane shear (crack surfaces are sheared relative to each other in a direction normal to the edge of the crack).

Mode III: Tearing or anti-plane shears (the crack surfaces move parallel to the leading edge of the crack and relative to each other).

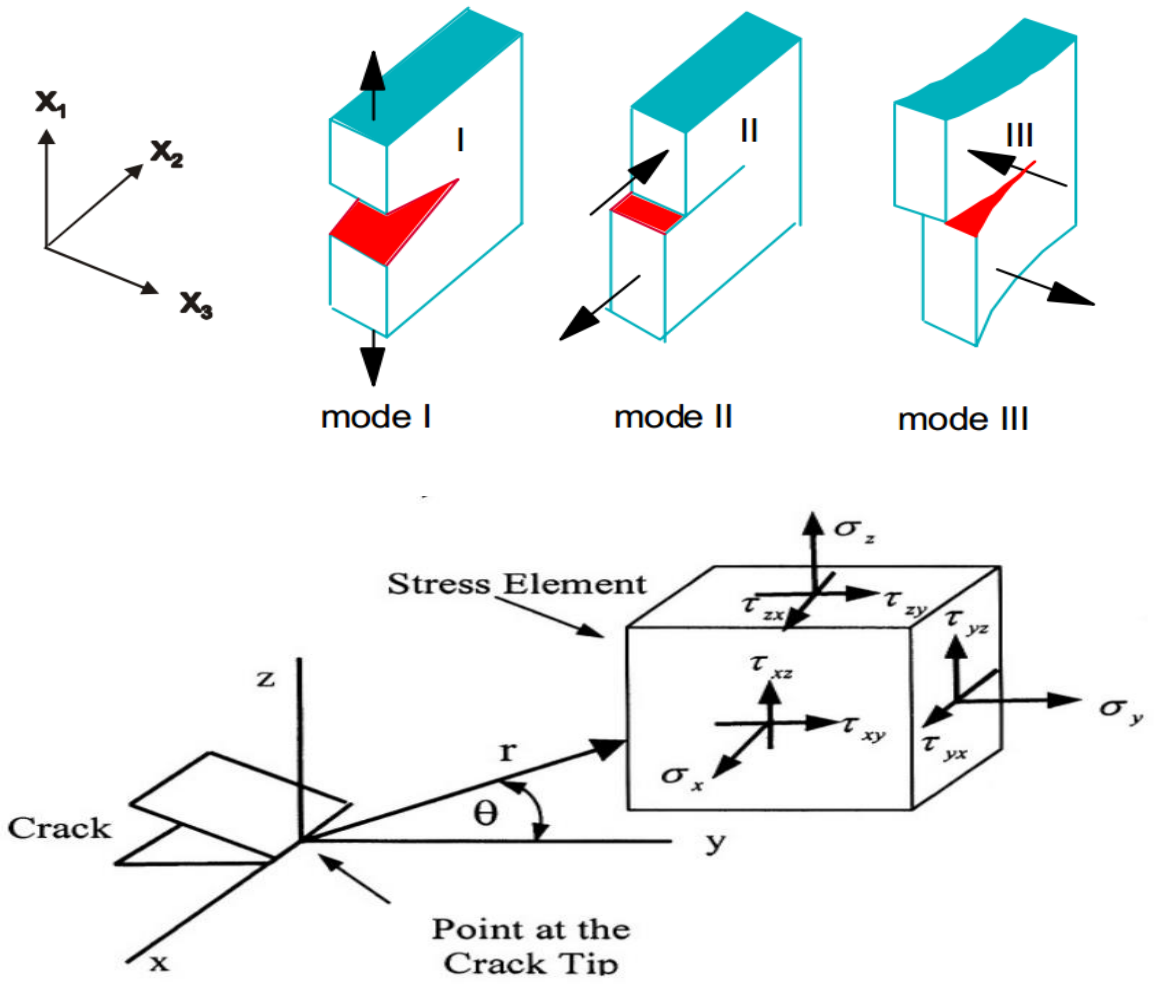

Figure4.1: stress loading modes and crack coordinate system [42]

N.B the wheel and rail interaction are sliding and rolling method so in this thesis Mode I is applied.

4.2 Crack Initiation and Propagation for Rail

The life of rail, in track, can be divided into two stages crack initiation and propagation. Crack initiation refers to the period of time (or the tonnage passing over the rail), but cannot be detected by existing inspection technique. Crack propagation refers to the period of time it takes a detectable defect to grow to a size that will fall under traffic. Cracks may initiate at or below the surface due to high traction forces that are resulted from fast motion of vehicles over the track. Sub-surface cracks propagate towards the rail surface and behave like original surface cracks after penetration [27].

In principle, the prediction of crack growth using fracture mechanics requires the following steps:

1) Identify the relevant crack growth properties (crack growth rate as a function of the stress intensity factor, fatigue threshold, fracture toughness, etc.) for the rail.
2) Determine the initial flaw size, shape, and location.
3) Determine the stress intensity factor solution as a function of crack size, shape, geometry, and loading.
4) Select a fatigue crack growth rate model and damage accumulation rule.
5) Propagate fatigue crack from initial flaw size to final (critical) flaw size.

4.3 Crack Growth Model of Rail

In general, many fatigue life analysis have applied the Miner's damage accumulation law or some specific to predict the probabilistic life of a metallic material, since the models accordingly represent the characteristics of the material. However, rail road companies usually use a crack size as the inspection results. Therefore, it is hard to deal with reflecting the results of the inspections and repair strategy in their approaches because they do not provide information about crack size.

4.3.1 Semi-Elliptical Crack Growth

The crack growth model used in this study is based on the Paris and Erdogan's law (crack growth rate is an exponential function of the stress intensity factor).Paris' law (also known as the Paris- Erdogans law) relates the stress intensity factor range to sub-critical crack growth under a fatigue stress regime. As such, it is the most popular fatigue crack growth model used in materials science and fracture mechanics [28].

The basic formula reads:

$$\frac{da_c}{dN} = C\Delta K^m \tag{4.2}$$

Where: - $a_c$is the crack length and N is the number of load (stress) cycles. Thus, the term on the left side, known as the crack growth rate, denotes the infinitesimal crack length growth per increasing number of load (stress) cycles. On the right hand side, C and m are material constants, and ΔK is the range of the stress intensity factor.

The formula was introduced by P.C. Paris in 1961. Being a power law relationship between the crack growth rate during cyclic loading and the range of the stress intensity factor, the Paris law can be visualized as a linear graph on a log-log plot, where the x-axis is denoted by the range of the stress intensity factor and the y-axis is denoted by the crack growth rate. Paris' law can be used to quantify the residual life (in terms of load cycles) of a specimen given a particular crack size.

The size of the semi-elliptical rail head crack can be expressed in terms of its area relative to the rail head area, which is equal to $3.1*e^{-5}mm^2$ for T50 rail[29]. That is, growth is calculated in terms of crack size in percent rail head area (%HA).$A_{crack} = \frac{\pi x a_c x b_c}{2}$is used to calculate the area of the semi-ellipse. The initial crack sizea_i is assumed to be 10%HA, which roughly corresponds to the smallest defect size that non-destructive testing equipment can detect. Moreover, the results of the different researches suggest growth of a semi-elliptical head defect for rails range from 10 to 50% [29]. In this thesis, 10% HA is employed as the elliptical crack size for the T50 rail. The dimension of elliptical crack is taken as 0.01mm for the major axis and 0.005mm for the minor axis respectively.

4.3.2Determination critical crack size of rail

The propagation of a crack is driven by the stress field that develops ahead of the crack tip. In fracture mechanics, the stress and strain fields can be characterized by parameters such as the stress intensity factor, K, under elastic conditions. The stress intensity factor (K) is used in fracture mechanics to predict stress intensity near the tip of a crack caused by a remote load or residual stresses.

According to Linear Elastic Fracture Mechanics under constant amplitude loading, stress intensity factor (ΔK) can be estimated as:

$$\Delta K = K_{max} - K_{min} \Delta K = Y \Delta\sigma \sqrt{\pi a_c} \tag{4.3}$$

Where, Y is the geometric correction factor and $\Delta\sigma$ is the tensile stress range, also called the far field stress range and $a_c$is the crack size. At any point along the boundary of the elliptical crack, the mode I stress intensity factor can be written as:

$$K = \frac{\sigma\sqrt{\pi a_c}}{\varphi} \sqrt[4]{\left(\frac{a^2}{c^2} Cos^2\theta + sin^2\theta\right)} \tag{4.4}$$

Where, σ is the far field stress, a is the crack size, $\theta$is the angle that defines any point around the perimeter of the elliptical crack, and φ is the elliptical integral of the second kind, given by

$$\varphi = \int_0^{\pi/2} \sqrt{\left(1 - \left(1 - \left(\frac{a}{c}\right)^2\right) sin\theta\right)} d\theta \tag{4.5}$$

An empirical expression that can describe the quantity φ of above equation for different crack depth to crack length aspect ratios, a/c, is given by;

$$\varphi^2 = 1 + 1.464 \frac{a^{1.65}}{c^{1.65}} \quad for \ {}^{a}/_{c} \leq 1$$

$$\varphi^2 = 1 + 1.464 \frac{c^{1.65}}{a^{1.65}} \quad for \ {}^{a}/_{c} > 1$$

Where the crack is circular, where the aspect ratio a/c=1, the value of stress intensity factor around the crack front is a constant. From above equation, the stress intensity factor corresponding to an elliptical crack with aspect ratio a/c ≤1) can be written as:

$$K_i = \frac{1.12\sigma\sqrt{\pi a}}{\varphi}$$

$$K_i = 0.806\, \sigma\sqrt{a_c} \tag{4.6}$$

Where: - the quantity

φ = 2.464

4.3.2.1 Crack Insertion and Meshing

The finite element method was used to calculate the stress intensity factor due to the complexity of the rail geometry. Finite element codes must meet two requirements to resolve the singular stress at the crack tip. The first requirement is the element size: the new elements used to populate the crack region must be smaller than the existing mesh to calculate the stress-intensity factors accurately. However, the new elements must be large enough to address singularity at the crack tip. The second requirement is the element number: the number of elements around the crack tip influences the circumferential stress distribution. In general, the stress result is more accurate with more elements; but the results quality is compensated if the crack tip is over crowded with high aspect ratio elements. In order to meet the requirements by generating a smooth transition from the tip of the crack to the unmodified mesh, the ANSYS 14.5 insert "a rosette of crack-tip elements" that can be subdivided automatically and repeatedly into triangular and quadrilateral elements.

The Single front elliptical cracks are defined by entering the semi-axes lengths ($a_c$andb_c) which are 0.01m and 0.005m respectively. Once a flaw (crack) is defined, it was inserted (translated and rotated) into the proper location relative to the unflawed body of the rail as shown below.

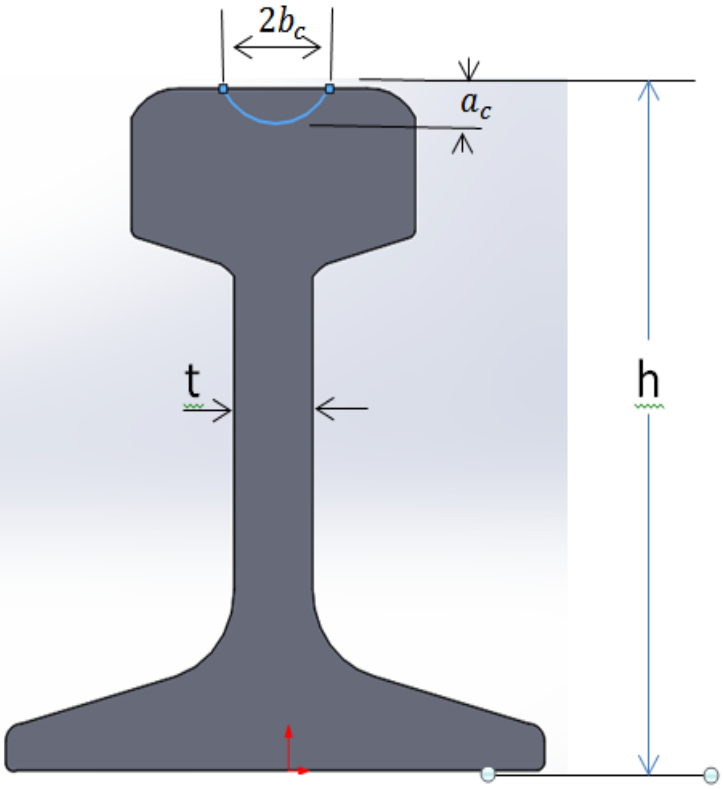

Figure4.2: Semi-elliptical crack model

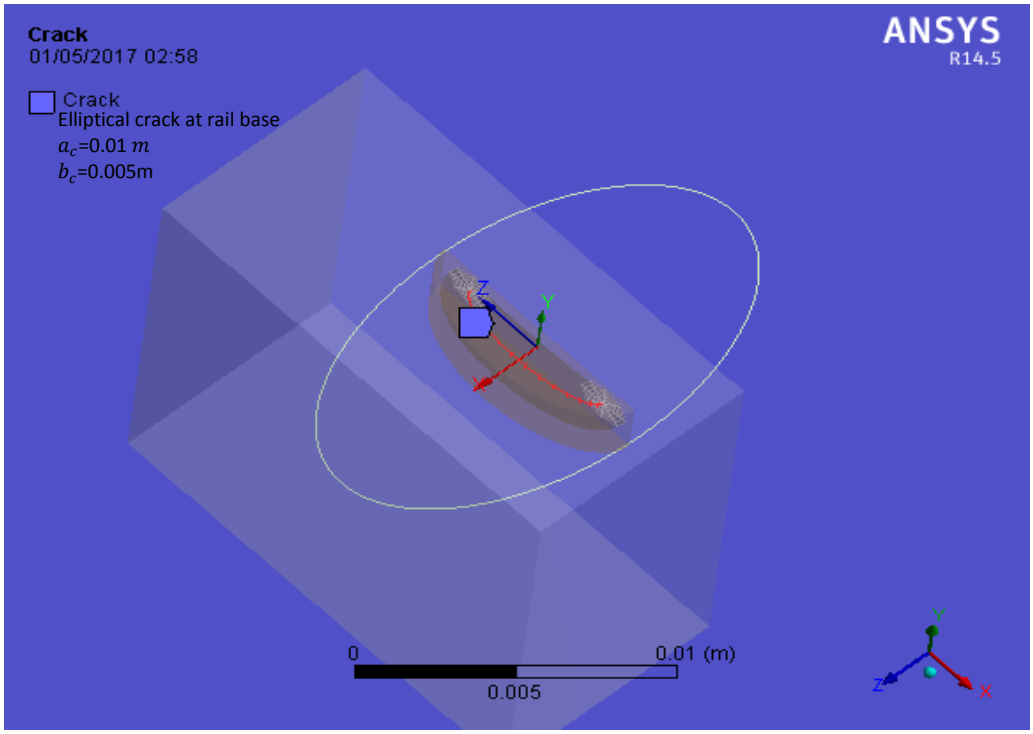

Figure4.3: Location and orientation of elliptical crack at rail base.

The crack geometry is inserted into the model geometry first, represented by the Doing geometric intersections status. Once the crack geometry has been inserted, trimmed, and tied to the rail model geometry, surface and then volume meshing occurs. The final mesh is smoothed to improve the element quality.

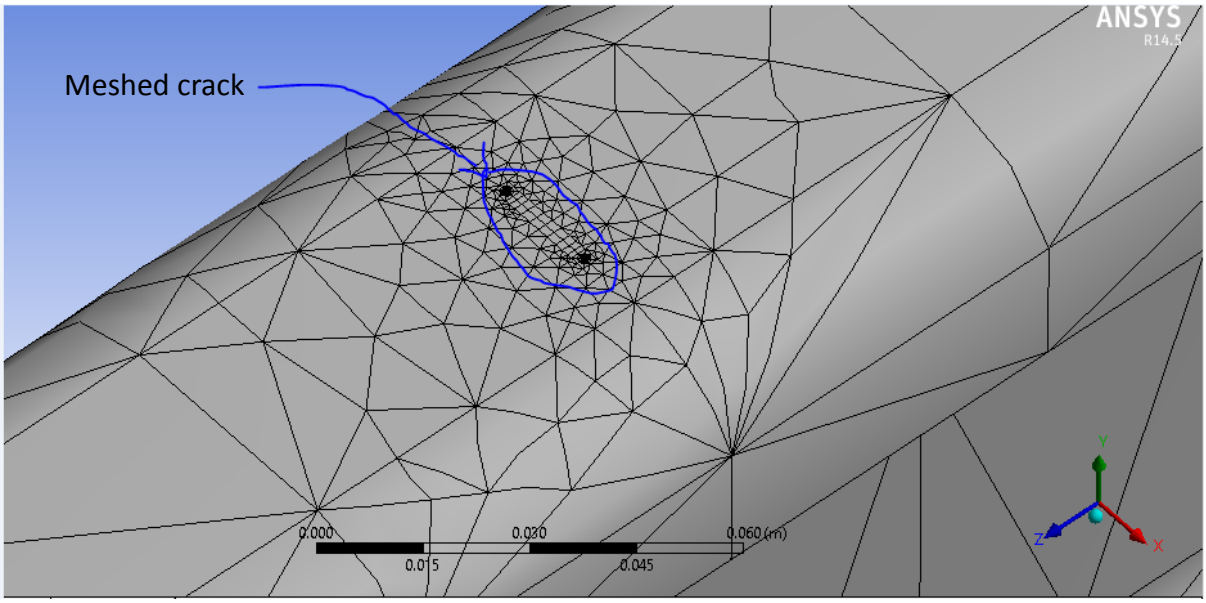

Figure4.4: Meshed rail model with crack at rail head

4.3.2.2 Loading and Boundary Conditions

Fixed boundary condition is applied to the rail at the bottom of the foot. Pressure is applied on the finite element model, approximated as multiple uniform pressures over contact patch area with inserted crack.

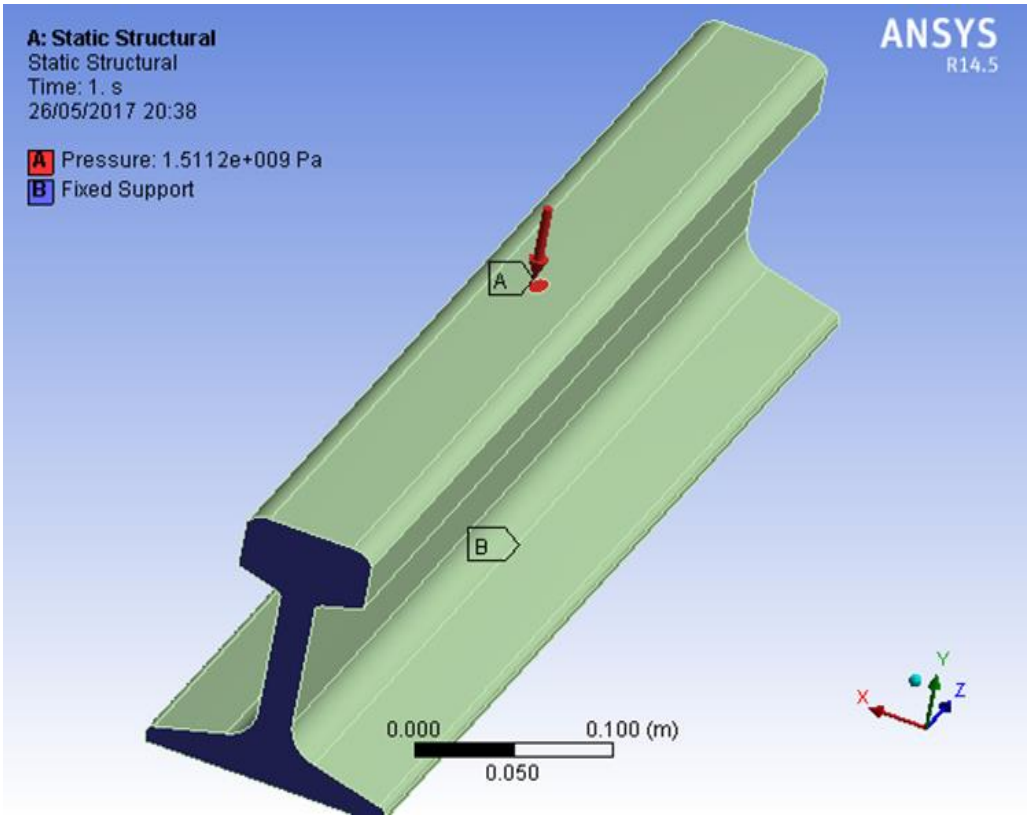

Figure4.5: Rail boundary conditions and input data

4.3.2.3Static crack stress analysis results

Fracture that occurs over a very short time period and under simple loading conditions (static i.e. constant or slowly changing) is considered here. Static crack analysis is a static (single step, no crack growth) deformation analysis. The stress intensity factor (K) is used in fracture mechanics to predict stress intensity near the tip of a crack caused by a remote load or residual stresses. This analysis is wanted to compute stress-intensity factors for this crack without performing any crack growth. The Stress intensity factors results are negative because of the crack propagate in down word direction.

1) **Stress intensity factors I (K_I)**

The parameterK_I is called the stress intensity factor which is the crack driving force and its critical value is a material property known as fracture toughness, which in turn, is the resistance force to crack extension. The maximum value of K_I **is -1.5318e7**$\mathbf{Mpa/\sqrt{mm}}$

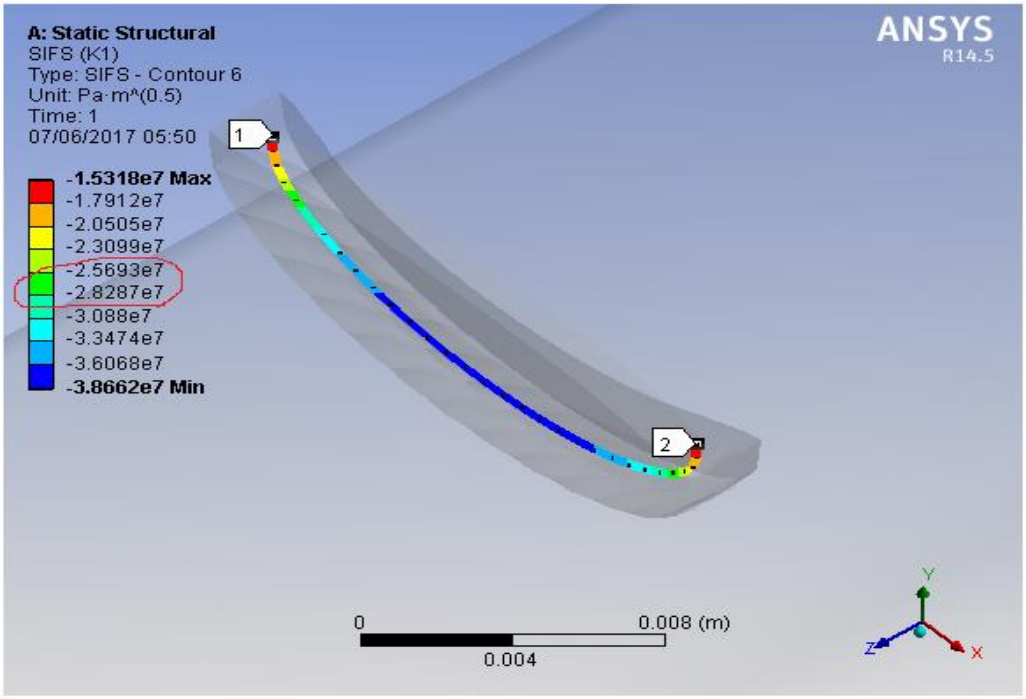

(a)

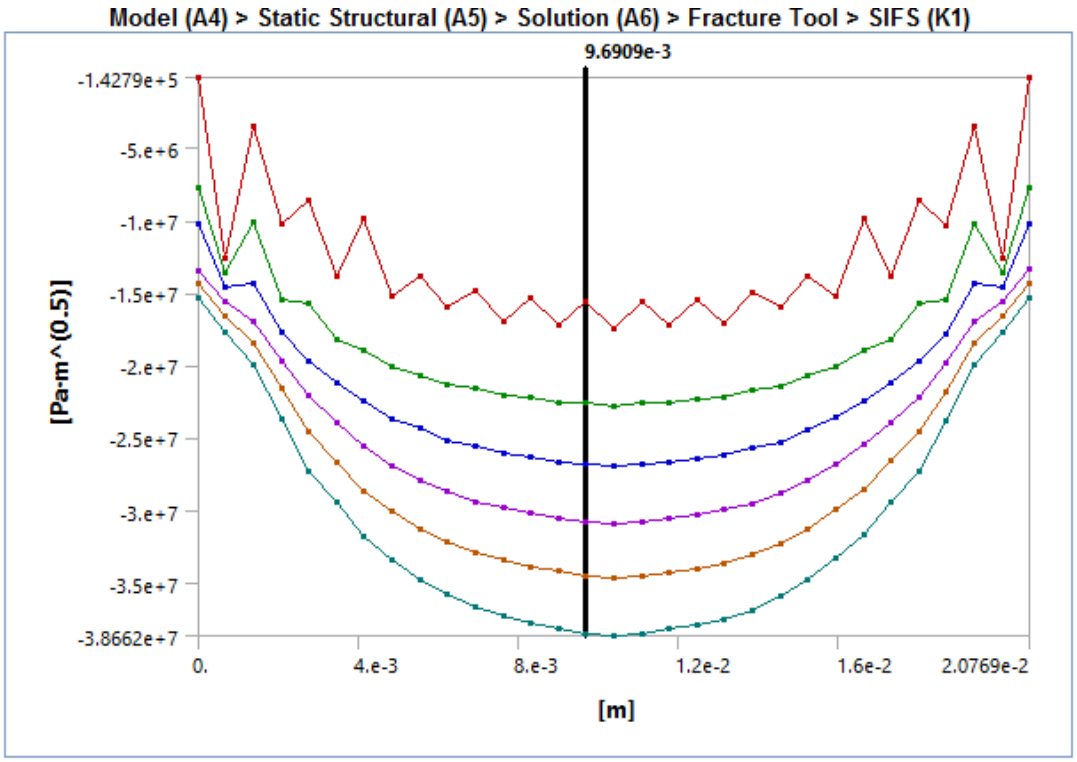

(b)

Figure4.6: (a) Stress intensity factor, K_I(b) Graph of SIF I (K_I) with respect to normalized distance along crack front

2) **Stress intensity factors II (K_{II})**

The maximum value of K_{II} **is -9.161e6**$\text{Mpa}/\sqrt{mm}$

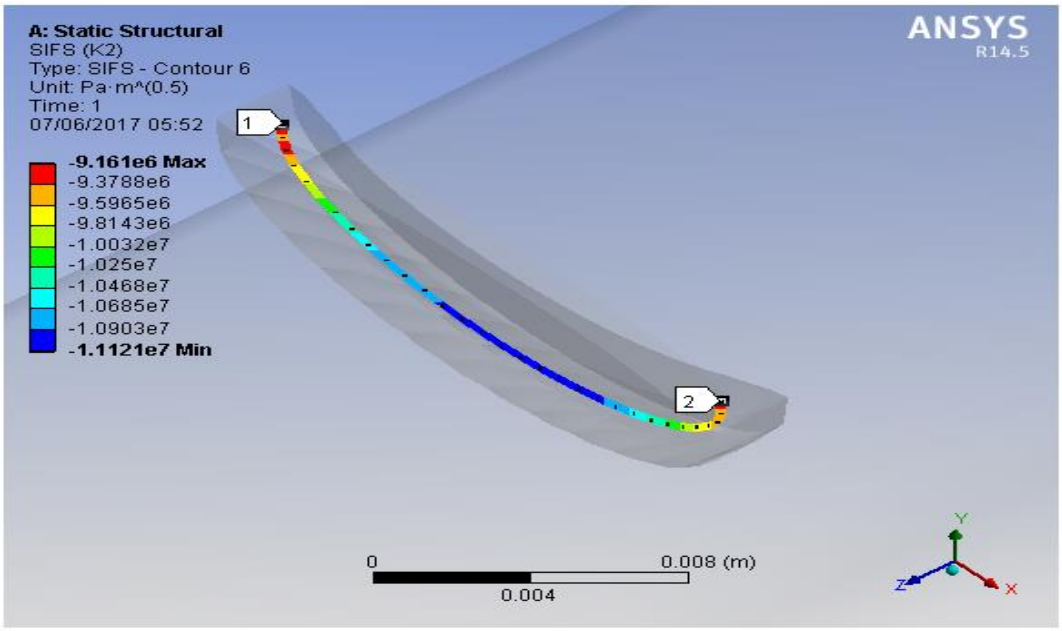

(a)

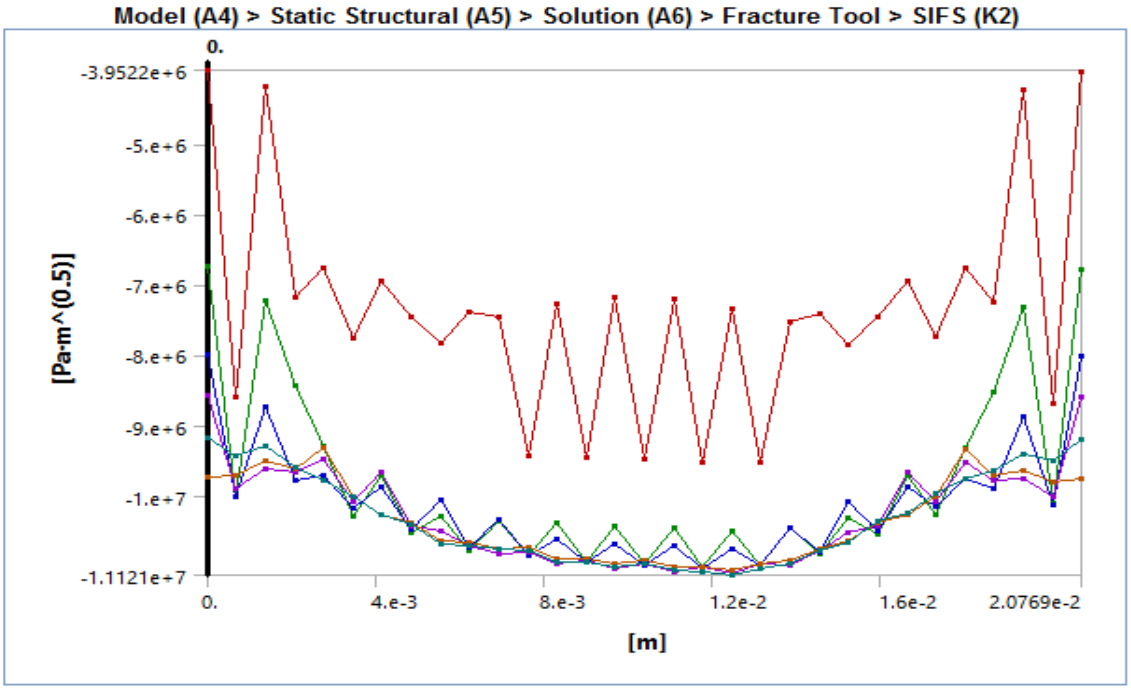

(b)

Figure4.7: (a) Stress intensity factor,K_{II}(b) Graph of SIF II (K_{II}) with respect to normalized distance along crack front.

3) Stress intensity factors III(K_{III})

The maximum value of K_{III} **is 1.24e7**$\text{Mpa}/\sqrt{mm}$

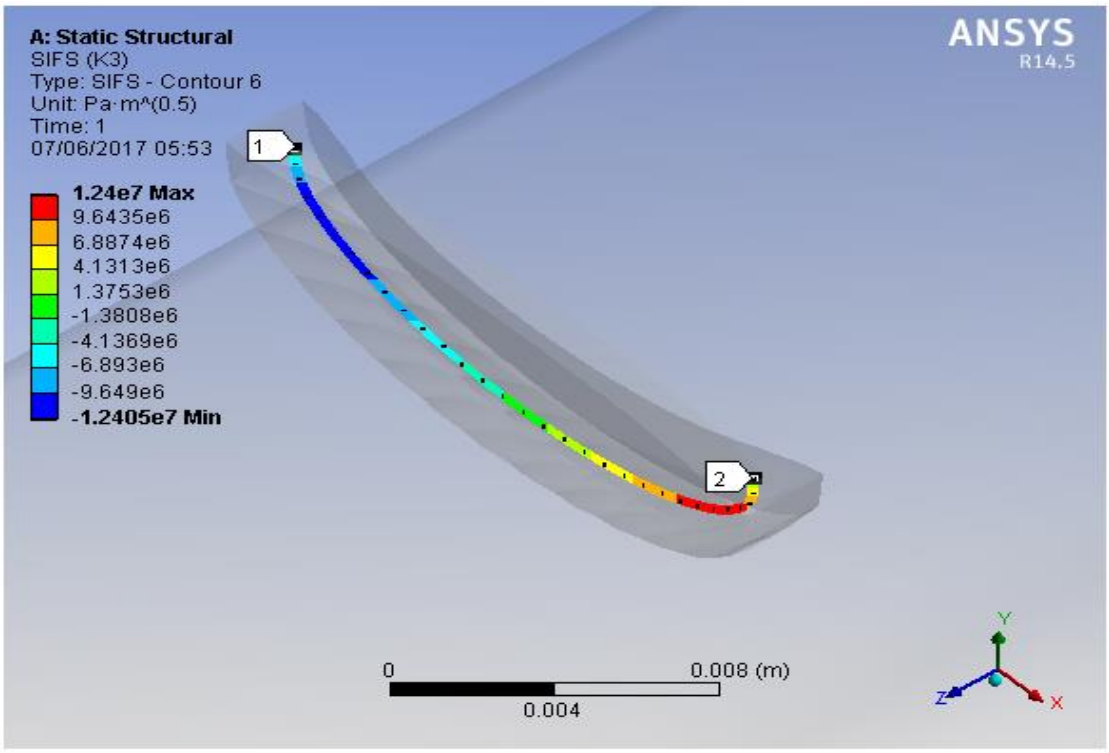

(a)

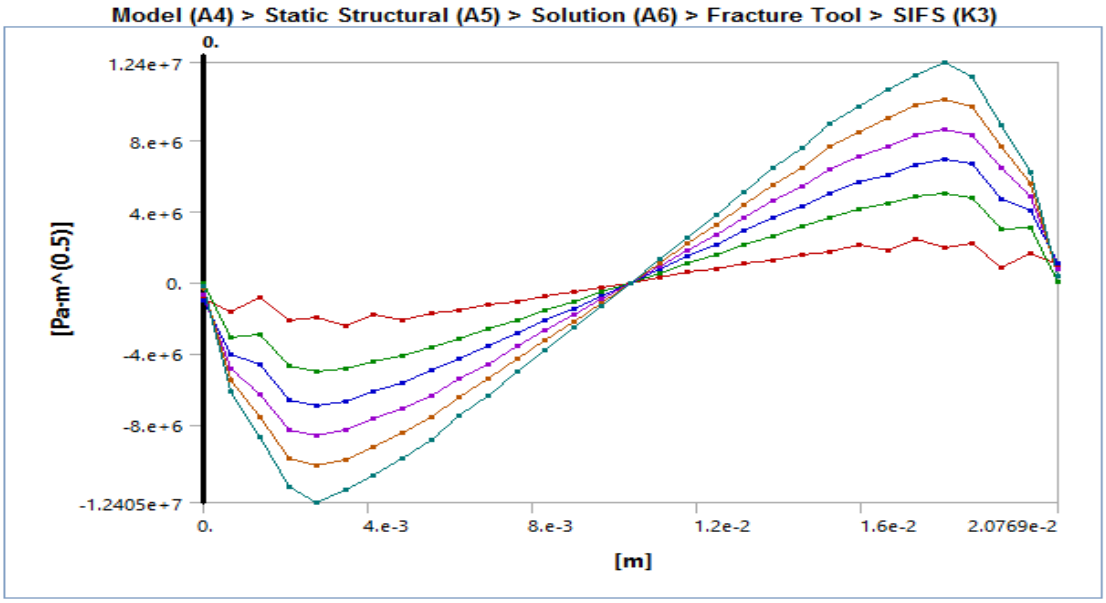

(b)

Figure4.8: (a) Stress intensity factor,K_{III} (b) Graph of SIF II (K_{III}) with respect to normalized distance along crack front

4) J -integral

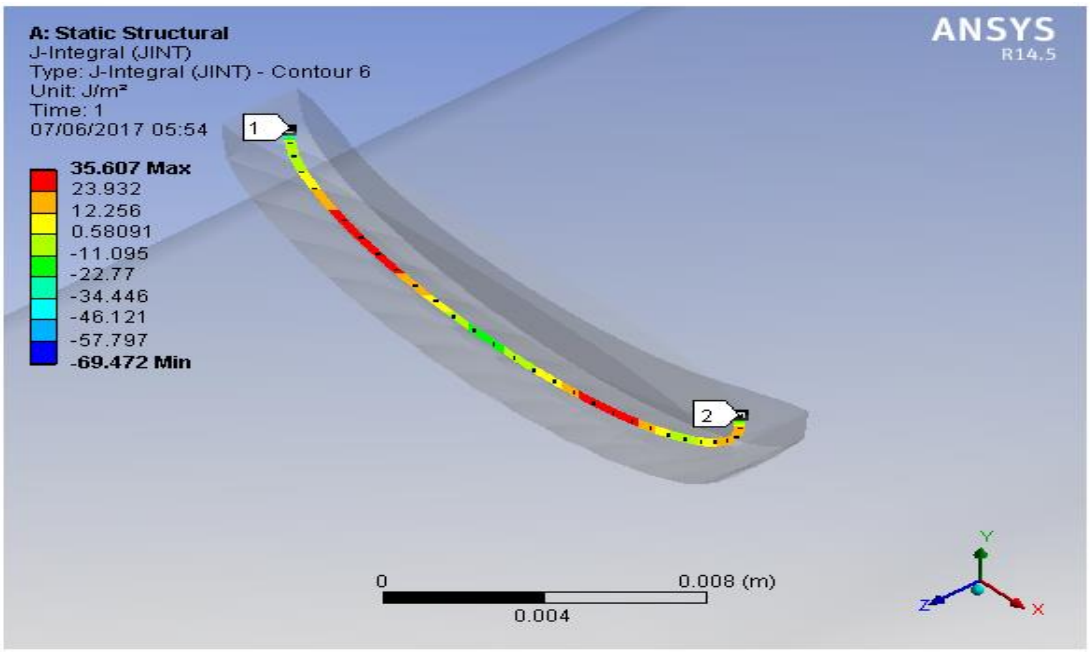

(a)

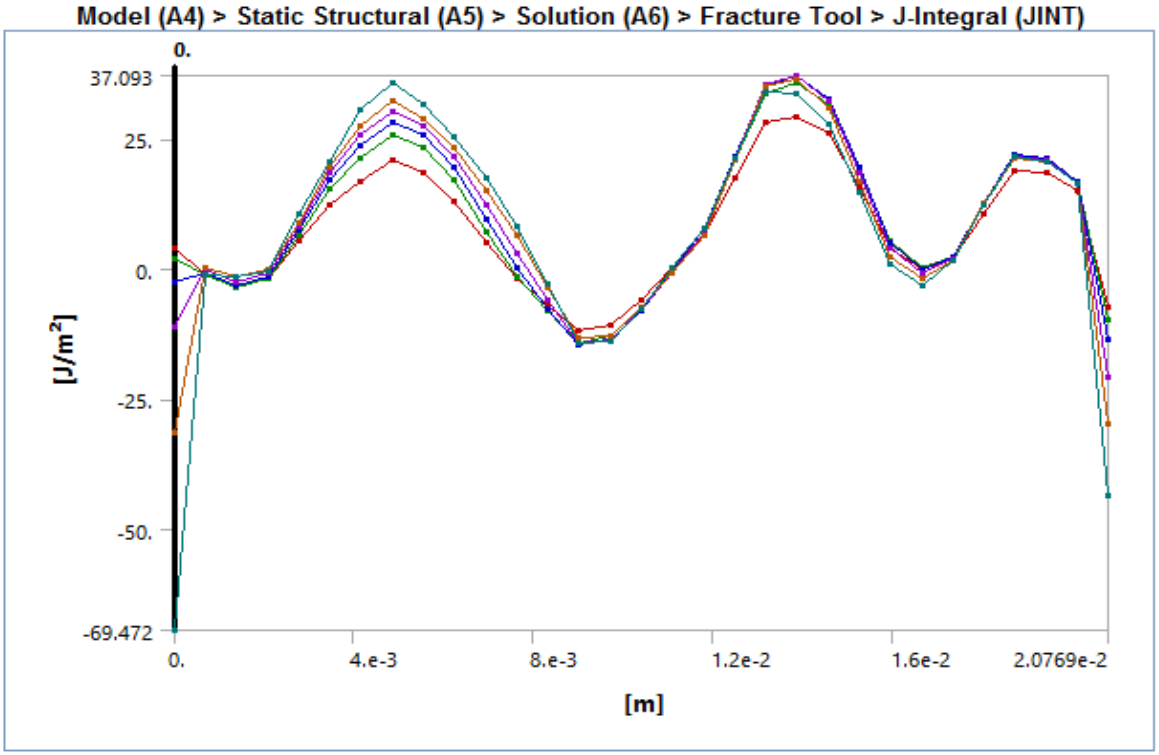

(b)

Figure4.9: J-integral with respect to normalized distance along crack front

4.4. Fracture Toughness

In materials science, the fracture toughness$K_{Ic}$is a property which describes the ability of a material containing a crack to resist fracture. The subscript *I* denotes mode I crack opening under a normal tensile stress perpendicular to the crack. Fracture toughness is a quantitative way of expressing the resistance of a material to brittle fracture when a crack is present. It is independent of the size and geometry of the cracked body under certain conditions. The materials with higher values of fracture toughness are more likely to undergo a ductile fracture; however, the materials with low value fracture toughness usually undergo a brittle fracture [30]. The largest crack a structure can sustain under specific strength requirements can be predicted through this critical value of the SIF where the crack propagation becomes unstable. The mechanical properties and fracture toughness of rail steel is determined by static tensile experiment using MTS materials testing system of electronic discharge machining (EDM).

The national standards of the people's republic of China manual recommend the following for the fracture toughness of rail steel: 'the mean value of fracture toughness $K_{IC}$of rails shall be 26MPa√m [30]. So, in this thesis, a fracture toughness mean value of 25.693MPa√m and 28.287MPa√m are taken from stress intensity factor, K_1so the mean fracture toughness value for the T50 rail of national railway network of Ethiopia is 27MPa√m.

$$a_{ch} = \frac{1}{\pi}\left(\frac{K\varphi}{1.12\sigma_c}\right)^2 = \frac{1}{\pi}\left(\frac{27 * 2.46}{1.12 * 1511.22\text{MPa}}\right)^2 = 5mm$$

By using equation 4.6 $K_i = 0.806\ \sigma\sqrt{a_c}$the stress intensity factor calculated in below table

Table 5: Stress intensity factor vs. crack length

Crack size, a(mm)	Stress intensity factor (mpa/$\sqrt{mm}$
0.0	0
0.5	861.28
1	1218.04
1.5	1491.78
2	1722.56
2.5	1925.89
3	2109.7
3.5	2278.74
4	2436.08
4.5	2583.853
5	2,723.62

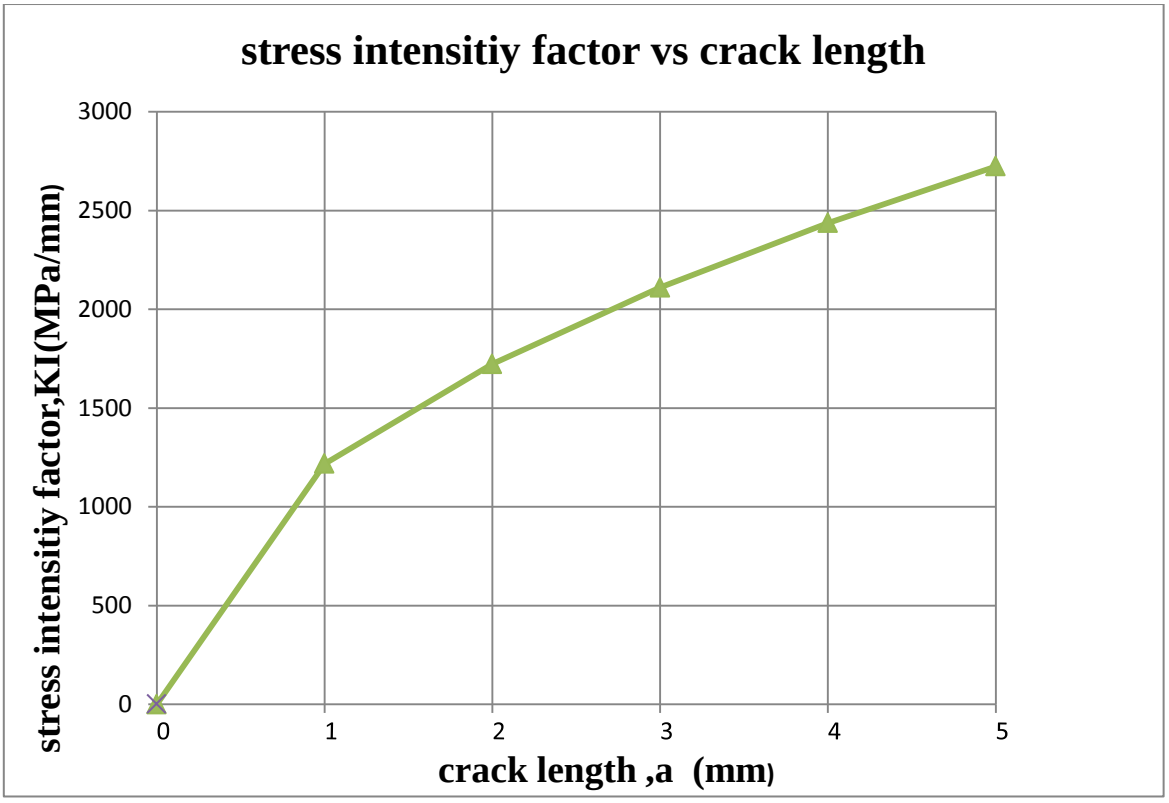

Figure4.10: Stress intensity factor versus crack length

4.5 Fatigue life

It is well established that fatigue is essentially a two stage process; crack initiation and crack propagation. The crack initiation stage is governed by number of load cycles required for a fatigue crack to initiate and to become a potential stress raiser. However, crack propagation stage comprise of the loading cycles required to grow the initiated crack until the final failure of the structure is reached.

A fatigue life analysis is performed based on Paris law. As mentioned above, the Paris law states that the crack growth rate is an exponential function of the stress intensity factor, ΔK:

$$\frac{da}{dN} = C\Delta K^m = C\left(\Delta\sigma Y\sqrt{\pi}\right)^n$$

Where: - C and m are the material specific input parameters. Generally, for metals, values of m ranges from 2.5 to 3.5 and the C values ranges from $1* 10^{-9}$to $1*10^{-11}$[31].So, m=3 and $c=1*10^{-11}$ are taken as the specific input parameters in this thesis for the T50 rail of national railway network of Ethiopia is the basic understanding of the fatigue strength behaviour of the rail. For calculation of fatigue life of rail σ=1511.22MPa at the rail head are taken.

$$K_1 = \left(1.12\sigma\sqrt{\pi a}\right)\Big/_{\varphi} = 0.806\ \sigma\sqrt{a_c}$$

$$(\Delta K)_2 = 0.806 * 1511.22 * \sqrt{0.0005} = 27.23$$

$$(\Delta K)_4 = 0.806 * 1511.22 * \sqrt{0.001} = 38.51$$

$$\frac{da}{dN} = C\Delta K^m$$

$$(da/dN)_2 = 10^{-11}(27.22)^3 = 20{,}204.27 * 10^{-11}$$

$$(da/dN)_4 = 10^{-11}(38.51)^3 = 57{,}146.31 * 10^{-11}$$

Mean of $(da_c/dN)_2$ and $(da/dN)_4$ = $38{,}675.28 * 10^{-11}$

$dN = 0.0005/38{,}675.28 * 10^{-11} = 1{,}292.81$

Table 6: Crack length vs. no. of cycles for rail head

Initial Crack length (a_o)(mm)	Increment of crack growth Δa_i	Final Crack length (a)(mm)	ΔN (cycles)	N (cycle)
0.5	0.5	1	1,292.81	1,292.81
1	0.5	1.5	1,233.57	2,526.38
1.5	0.5	2	1,125.20	3,651.58
2	0.5	2.5	1,032.19	4,683.77
2.5	0.5	3	956.35	5,640.12
3	0.5	3.5	894	6,534.12
3.5	0.5	4	841.99	7,376.11
4	0.5	4.5	797.85	8,173.96
4.5	0.5	5	759.85	8,933.81

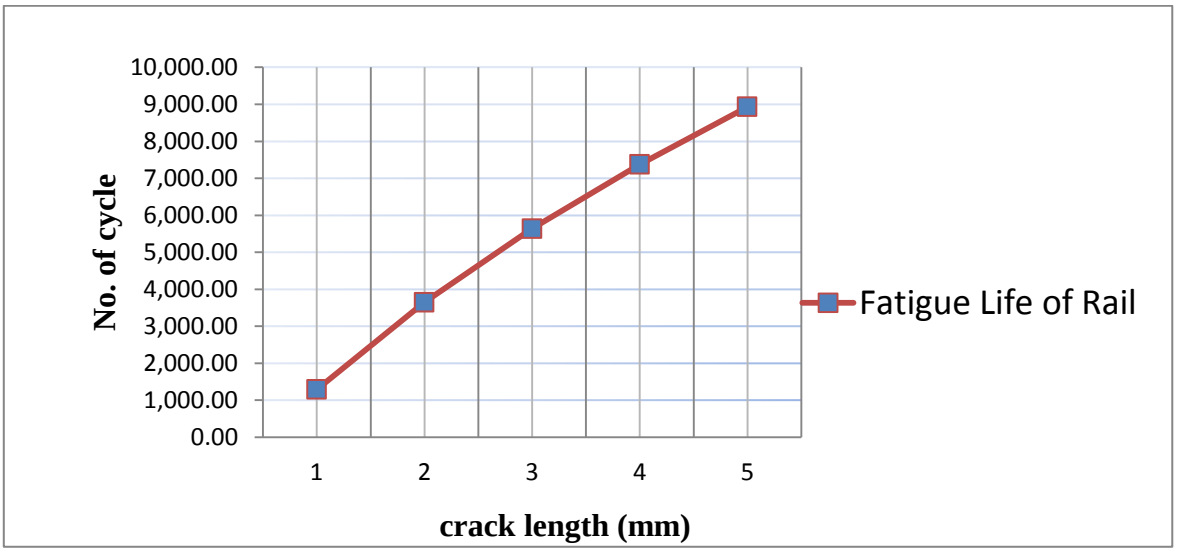

Figure4.11: Fatigue life of rail

The equivalent alternating stress is increases as the load increases. In contrary as the load increases, the crack length is increasing that means the fatigue life of rail is decreasing , in general means the more load is applied the fatigue life of the rail will be smaller and smaller. It is seen from the table 6 and figures 4.11 that, fatigue life of rail is concerned, the suitable cyclic axle load and proper maintenance before crack initiate and propagate may be regarded as the best possible life improvement operation.

CHAPTER FIVE: - RAIL INSPECTION AND MAINTENANCE STRATEGY MODEL

5.1 Introduction

Inspection and maintenance today is viewed as a value adding concept; because it contributes efficiency to the company's strategic objective in profitability and competitiveness. Achieving more efficient maintenance depends on the capability of the implemented inspection and maintenance policy to provide and employ effectively the relevant information about the factors affecting the life of rails being considered [32].

Inspection and maintenance of rails not only increases the life length but may also reduce the failures and degradation rates. Inspection (in the operation phase) is a maintenance activity carried out at predetermined time intervals in order to reduce the probability of failure (or the performance degradation) of the rail. The inspection cost increases when the inspection interval is shortened (or the inspection frequency is increased), as inspection is one of the cost elements.

Although detection of broken rails using the passive approach, based on rail response from the principles of engineering mechanics, is possible, most existing technologies rely on the active method of transmitting and receiving signals; these technologies usually require trackside infrastructure that is expensive to maintain if not install[33].

5.1.1 Damage detection techniques

In general, the basic premise behind these active methods of structural damage identification is that the defects cause changes in structural physical properties, which will, in turn, alter structural response characteristics such as vibration responses and wave propagation characteristics in structural solids, among others. Hence, by monitoring response signatures through the use of various measurement sensors and data acquisition technologies, the current condition of the structural system concerned can be determined.

The damage identification techniques generally involve four levels of identification processes. These included (from lowest level to highest level) [34].

- Detection of the existence of any defects
- Identification of the location of the defects, if they exist
- Determination of the severity of the defects
- Determination of the remaining service life of the infrastructure concerned.

In general, there exist three main categories of techniques currently used for damage identification and condition monitoring of structures and solids.

These include:

- visual inspections
- Non-destructive testing (NDT) technologies such as acoustic emissions or ultrasonic methods, magnetic field methods, radiography, eddy current techniques, thermal field methods, dye penetrate, fibre optic sensors of various kinds
- vibration-based 'global' methods.

Figure5.1: Different type of damage detection techniques [34].

Both visual and NDT-based methods offer limited capabilities to conduct 'global' structural damage condition investigation in common structural systems such as bridges and buildings. The successful implementation of these inspection methods generally requires the regions of the suspected damage to be known as a first step, and be readily accessible for physical inspection. As a result, these methods can be costly, time consuming and ineffective for large

and complex structural systems such as the rail track. However, it is important to mention that visual inspection and NDT-based technologies are the primary techniques used for defect identification in structural solids, and are effectively used in specialised disciplines, such as in the railways.

In the context of this chapter, the technologies for high speed detection of broken rails, rail cracks and surface faults should be able to not only detect the existence of rail defects or breaks, but also provide reliable predictive information regarding the location and severity of the rail defects or breaks, so that appropriate real-time safety measures can be implemented by railway managers.

5.2 The Frequency of Rail Inspection and Maintenance

According to the predicted traffic volume in the feasibility study of Some National Railway Network of Ethiopia, the forecasted number of trains varies from section to section. Similarly, the annual traffic density for the National Railway Network of Ethiopia is taken as 22.67MGT (Million Gross Tones). So, to determine the number of trains per day, we use the Vopecenter empirical formula which is as a function of annual traffic density as follows:

$$X \text{ (No. Of trains per day)} = T/0.006312/365 = 10$$

Finally, the fatigue life of rail as a function of MGT (Million Gross Tones) is obtained as follows:

Assume one train passes a certain track section two times per day. So, the total number of cycles per year for loaded standard vehicle with four axles or eight wheels is

$$8*(10*365) = 29{,}200 \text{ cycles/year.}$$

$$29{,}200 \text{ Cycles} = 22.67 \text{ MGT}$$

The frequency of rail inspection tends to vary from one railroad to another, yet it is usually based on either time or traffic tonnage. Railroad companies have evolved their rail inspection schedules empirically, based on long field experience. Rail defect management refers to the development and implementation of strategies to control the risk of rail failure. Rail defect inspection should be scheduled such that the occurrence of broken rails is minimized. The primary method to control the risk is a rail inspection through non-destructive evaluation and is a replacement of rails based on the remedial action plan as well as evaluation results. From the previous crack analysis, with the assumption of 22.67MGT (Million Gross Tones) annual traffic density the fatigue life of rail based on the maximum critical number of cycles for rail

head is taken as 6.9MGT (Million Gross Tones). Therefore, the frequency of rail inspection required will be:

Frequency of rail inspection per year $= \frac{6.9MGT}{22.67MGT} = 0.30$

I.e. number of rail inspection per year should be three or (in every four months the rail needs inspection).

Table 7: Recommended rail defect inspection frequencies

Annual Day-to-Day Traffic (Car Movements	Inspection Frequency
1 million gross tons (MGT) or more (greater than 7,200 car movements per year)	3 years or 3 MGT, whichever is less
0.5 to 0.99 MGT (3,600 to 7,200 car movements per year)	5 years or 5 MGT, whichever is less
Less than 0.5 MGT (less than 3,600 car Movements per year).	6 years or after a rail break

According to Rail road track standards by US Departments of the Army and the Air Force the recommendations are listed above. Therefore, for the value we get at the transition section i.e. 6.9MGT or 8933.81 Cycles as it exceeds 1 million gross tonnes (MGT) or 7200 car movements per year the recommended rail defect inspection frequency is 3 years or 3 MGT whichever is less. Generally, from all the above recommendations we choose the one which give us the minimum period of inspection interval. Therefore it is recommended to inspect the rail every three month to increase the service life of the rail and to minimize expected accidents.

Table 8: Remedial Action Table in JR East

Types of Defects	Criteria [mm]	Remedial action
Vertical split head	$5 \leq a < 15$	Marking for check
	$2.54 \leq a < 30$	Apply bolted joint bar and plan to replace
	$30 \leq a$	Replace immediately
Split web	$2 \leq a < 6$	Marking for check

	$6 \leq a < 10$	Apply bolted joint bar and plan to replace
	$10 \leq a$	Replace immediately
Broken Base	$a < 3$	Apply bolted joint bar and plan to replace
	$3 \leq a$	Replace immediately
Bolt-hole crack	$a < 5$	Marking for check
	$5 \leq a$	Replace immediately

The crack at the rail head was obtained to be 5mm, so according to the remedial actions recommended by the Japanese Railway company, since a $\geq$ 5mm the rail should bemarking for check.

Table 9: Remedial action Table in DOT

Types of Defects	Criteria [mm]	Remedial action
Vertical split head	$2.54 \leq a \geq 5.08$	Limit operating speed over defective rail to 48 [km/h]
		Inspect the rail 30 days after it is determined to continue the track in use
Split web	$10.16 \leq a$	Limit operating speed over defective rail to 48 [km/h]
		Inspect the rail 30 days after it is determined to continue the track in use
Broken Base	$2.54 \leq a \geq 15.24$	Apply joint bars bolted within 10 days after it is determined to continue the track in use
		After applying the jointed bars, limit operating speed to 80 [km/h]
Bolt-hole crack	$2.54 \leq a \geq 3.81$	Limit operating speed over defective rail to 48 [km/h]
		Inspect the rail 30 days after it is determined to continue the track in use

JR East set up rules by which the track engineers have to replace the rail at 400 Million Gross Tones (MGT) with new one.

According to US Department of Transportation (DOT), since the crack is between 2.54 and 5.08mm it is recommended to inspect the rail 30 days after it determined to continue the track in use.

5.3 Rail Defect Management program

Research into broken rail detection was one of the main objectives of an international cooperative research program for railway organisations from five continents, organised under the UIC umbrella to develop the Rail Defect Management (RDM) program. It included seven project elements [35]:

- Benchmarking flaw statistics, current inspection systems, and effectiveness
- Inspection technology improvement
- Flaw growth rate prediction
- Remaining service life/repair potential
- Broken rail detection system
- Safety aspects and considerations
- Defect management strategies.

The project team members included: AAR/TTCI, East Japan Railway Company, India Railways, Queensland Rail (Australia), Spoornet (South Africa), and China Academy of Railway Sciences. Each RDM member organisation conducted particular tasks of the RDM program:

- East Japan Railways have undertaken improved vehicle-borne ultrasonic testing using sliding and rotating wheel probes, enhanced probe guidance, greater probe scanning area, and improved data processing.
- The China Academy of Railway Sciences has targeted vehicle-borne ultrasonic inspection at speeds up to 80 km/h (about double current systems).
- AAR focused on NDT technologies such as low-frequency eddy current, longitudinal guided ultrasonic waves, neural network analysis of ultrasonic signals, and laser generation and reception of ultrasonic signals.
- TTCI has evaluated three prototype systems: fibre optic cable bonded to the rail, strain gauge modules bonded to the rail, and an acoustic broken rail detection system.

- Spoornet and industrial partner IMT developed a solar-powered acoustic rail break detection system that uses acoustic transmitters and receivers clamped to the rails.
- India Railways' RDSO designed a test rig to apply loads to simulate vertical bending caused by passing

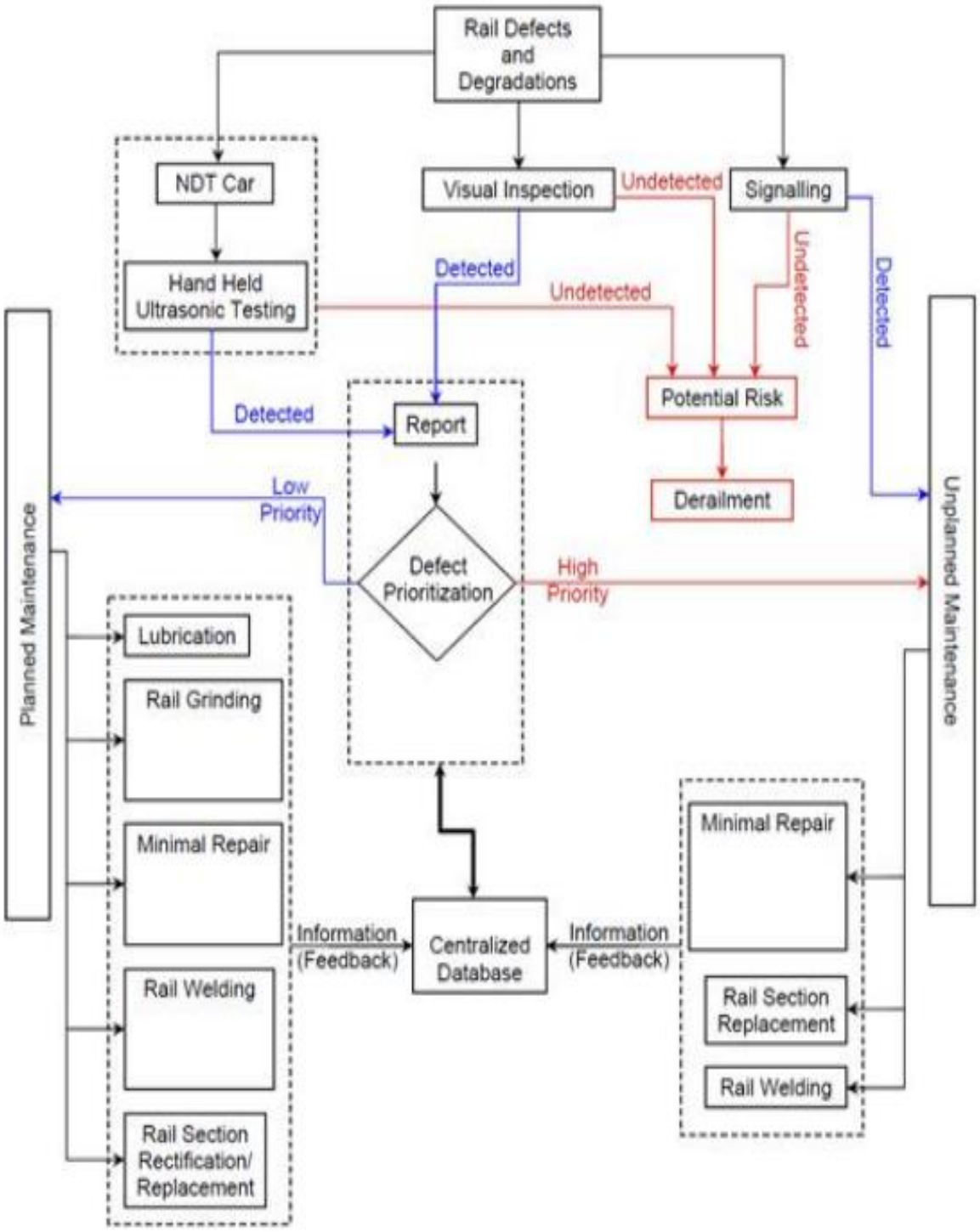

Figure5.2: Banverket's rail inspection and maintenance strategy flowchart [35].

CHAPTER SIX: - CONCLUSION AND RECOMMENDATION

6.1 Conclusion

This thesis discussed about rolling contact surfaces crack propagation analyses with an effective inspection and maintenance method. This will help to prevent the occurrence of rail failure by taking the required action at the right time, and extend the rail life expectancy, reduce the rail maintenance work.

The primary method to control the risk is a rail inspection through non-destructive evaluation and a replacement of rails based on the remedial action plan as well as evaluation results. To demonstrate the feasibility of the above method, first, a Linear Elastic Fracture Mechanics (LEFM) analysis which can predict a crack size in a rail head is performed. Therefore, based on the paper outputs with the above stress increment value the rail racks up to 5mm at the head, then the main conclusions obtained from the research are:

- The maximum stress distribution results obtained in the form of Von-Misses stresses is found to be 178.62MPa is less than the ultimate tensile strength of rail, so the rail can resist the pressure applied at the contact area.
- In conclusion as far as fatigue life of rail is concerned, the suitable cyclic axle load and proper maintenance before crack initiate and propagate may be regarded as the best possible life improvement operation.
- The rail should be inspecting in every three months (four times in a year).
- Based on the present rail crack value and the recommended remedial action plans the rail should be replaced when head crack of more than 5mm is observed.
- Apply jointed bars bolted within 10 days after it is determined to continue the track in use. Then after applying the joint bars, the operating speed should be limited to 80 km/h.
- Flow chart for rail inspection and maintenance management strategy has been adopted for National Railway Network of Ethiopia.

6.2 Recommendation

In order to minimize the occurrence of rail defect, an Ethiopian railway corporation rail should be inspecting frequently in every three months. It will reduce the risk of rail failures and the rate of derailment happening will be minimized. Predicting and preventive maintenance will help to increase the crack initiation and crack propagation and minimize the

cost of maintenance of rail change due to damage. Increasing the life of crack initiation and propagation means improving the total fatigue life of the rail itself. Additionally by using better strength material property than the AA light rail transit used, the fatigue life of the rail will be improved. At inspection time if the rail head crack value is greater than the critical crack value of 5mm, the rail should be maintain with respect to crack value.

6.3 Future Works

This thesis focuses on the rail surfaces crack propagation with an effective inspection and maintenance method analyses. However, several issues need further development and refinement to get more accurate output which approaches the real world scenario. Some of the recommendations for future works include:

- Considering a three dimensional (3D) finite element model with an increased length of the transition zone to get more accurate result and to better simulate the research problem with the real (practical) problem in the service life of the track structure.
- Considering other factors that affect track modulus, like environmental factors, sleeper suspension due to ballast flying, imperfection of rail joining and soon. For instance, on the rainy season the effect of water should be given higher attention because it lubricate the rail and highly contribute to the rail crack growth in addition to its effect on the sub grade by affecting its bearing capacity which intern contribute to track settlement.
- Further extend this work by doing Life Cycle Cost (LCC) analysis for the rail found on this transition section which includes optimal repair and maintenance schedule.

REFERENCE

[1]18th Euro Working Group on Transportation, EWGT 2015, 14-16 July 2015,Delft, The Netherlands ,and

[2] Wheel–rail interface handbookEditedbyR. Lewis and U. Olofsson,publishing limited by Woodhead.pdf

[3] Skyttebol, A. (2004): Continuous welded railway rails: Residual stress analyses, fatigue assessments and experiments. PhD Thesis, Chalmers University of Technology, Göteborg, Sweden.

[4] J E Garnham, D I Fletcher ,C L Davis, F J Franklin Visualisation and modelling to understand rail rollingcontact fatigue cracks in three-dimensions

[5] Guidelines to best practices for heavy haul railway operations : wheel and rail interface issues First Edition, First Printing, May 2001

[6] CRC for Rail Innovation High speed detection of broken rails, rail cracks and surface faults.SaurabhKumar ,Division of Operation and Maintenance Engineering ,Luleå Railway Research Center (JVCT) ,Luleå University of Technology, Luleå, Sweden ,

[7]Sawley, K. and Reiff, R. (2000): Rail Failure Assessment for the Office of the Rail Regulator. An assessment of railtrack's methods for managing broken and defective rails. Report of the Transportation Technology Centre Pueblo, Colorado, USA.

[8] Cannon, D.F., Edel, K.-O., Grassie, S.L. and Sawley, K. (2003): Rail defects: an overview. Fatigue and Fracture of Engng. Mat. andStruct. 26, 865-887. Bogdanski, S. and Brown, M.W. (2002): Modelling the three-dimensional behaviour of shallow rolling contact fatigue cracks in rails. Wear 253, 17-25.

[9] Meißner, K. and Hug, H. (2000): Detektion und Behandlung von Schienenfehlern in Gleisen und Weichen der DB Netz AG. In: Edel, K.-O. (ed.): Internationales Symposium „Schienenfehler", Brandenburg, Germany,November 2000, Proceedings, Paper 4.

[10]Skyttebol, A. (2004): Continuous welded railway rails: Residual stress analyses, fatigue assessments and experiments. PhD Thesis, Chalmers University of Technology, Göteborg, Sweden.

[11] Heshmata.Aglan and MahmoodFateh Fracture and Fatigue crack growth analysis of rail steels journal of mechanics of materials and structures vol. 2, no. 2, 2007.

[12] Ringsberg, J. W. and Bergkvist, A. (2003): On propagation of short rolling contact fatigue cracks. Fatigue & Fracture of Engineering Materials & Structures, 26(10), 969-983.

[13] Wong, S. L., Bold, P. E., Brown, M. W. and Allen, R. J.(1995). A branch criterion for shallow angled rolling contact fatigue cracks in rails. Wear, 191(1-2), 45-53.

[14]Canadinc, D., Sehitoglu, H. and Verzal, K. (2008): Analysis of surface crack growth under rolling contact fatigue. International Journal of Fatigue, 30, 1678-1689.

[15] Fisher, F. D., Daves, W., Pippan, R. and Pointner, P. (2006): Some comments on surface cracks in rails. Fatigue & Fracture of Engineering Materials & Structures, 29(11), 938-948.

[16] J.W. Ringsberg*, B.L. Josefson and A. Skyttebol Department of Applied Mechanics, Chalmers University of Technology, SE−412 96 Göteborg, Sweden

[17] Addis Ababa/Sebeta-Djibouti Railway Project (2012), Economic feasibility study, Addis Ababa.

[18] Lundberg, G. and Sjövall, H. (1958): Stress and deformation in elastic contacts. Department of Theory of Elasticity and Strength of Materials, Chalmers University of Technology, Publication no 4, Gothenburg, 60 pp.

[19] Timoshenko, S. P. and Goodier, J. N. (1970): Theory of elasticity, third edition. McGraw-Hill, Auckland, 567 pp.

[20] Johnson, K. L. (1985): Contact Mechanics. Cambridge University Press, Cambridge (UK), 452 pp.

[21] Iwnicki, S. (Editor, 2006): Handbook ofRailway Vehicle Dynamics. CRC Press, Boca Raton FL (USA), 535 pp.

[22] Esveld, C. (2001): Modern rail way track. 2nd ed., MTR-Productions, Zaltbommel, The Netherlands

[23] Selig E.T. and J.M. Waters, (1994). Variation of subgrade vertical stress and threshold stress with depth.

[24] Sadeghi J. and P. Barati, (2010). Evaluation of conventional methods in analysis and design of railway track system.International Journal of Civil Engineering. Vol.8,No.1

[25] Doyle, N.F., (1980). Railway track design: A review of current practice, Occasional Paper No.35, Bureau of Transport Economics, Australia, Canberra.

[26] Atkinson, B.K., Fracture Mechanics of Rock, pp. 534, Academic Press, London UK, 1987. Ch.1,2, 4.

[27] K. L. Johnson, "The strength of surfaces in rolling contact." Proc. InstMechEngng, 203, p. 151–163, 1989.

[28] P.Paris and F.Erdogan (1963), "A Critical Analysis of Crack Propagation Low," Journal of Basic Engineering, ASME, Vol.85, No.4, PP.528-534.

[29] David Y. Jeong, Michael E. Carolan, Hailing Yu and Benjamin Perlman, Fracture Mechanics and beam theory analysis of semi-elliptical cracks originating in the base of the rail, Cambridge, Massachusetts, USA, 2012.

[30] Andersen, T.M. (1999). Short Term Maintenance Planning.PhDThesis.Department of Marine Engineering, Norwegian University of Technology, Trondheim, ISBN 82-471-0408-3.

[31] N. Pugno, M. Ciavarella, P. Cornetti, A. Carpinteri., A generalized Paris' law for fatigue crack growth, Journal of the Mechanics and Physics of Solids, 54 (2006) pp. 1333–1349.

[32] Al-Najjar, B. and Kans, M. (2006). A model to identify Maintenance cost-effective decisions: a case study. International Journal of Productivity and Performance Management, 55(8), 616-637.

[33] Bahramin-Ghasrchami, K., Price, J.W.H. and Mathew, J. (1998). Optimum inspection Frequency for manufacturing systems. International Journal of Reliability Management, 15(3), 250-258.

[34] Rytter,A 1993, A vibrationbasedinspectionofcivilengineering structures, Doctoral Dissertation, Department of Building Technology and Structural Engineering,Universityof Aalborg, Aalborg, Denmark.

[35] Kalay, S., French, P., and Tournay, H. (2011). "The safety impact of wagon health monitoring inNorth America."Proc. of the World Congress on Railway Research, Lille, France, 2011.

[36] Schafer, DH&Barkan, CPL 2008a, 'A quantitativeanalysisoffactorsaffectingbroken rails', The William W Hay Railroad Engineering Seminar Series, Universityof Illinois at Urbana-Champaign.

[37] Taylor, R 2011, 'A system for broken rail detectionindependentof the signalling system', The Institution of Railway Signal EngineersInc, IRSE Australasia TechnicalMeeting,Sydney, March 18.

[38]Zerbst, U.; Lunden, R.; Edel, K.-O.; Smith, R.A.:Introduction to the damage tolerance behaviour of railway rails In: Engineering Fracture Mechanics (2009) Elsevier

[39] Ringsberg, J. W. (2001): Life prediction of rolling contact fatigue crack initiation. International Journal of Fatigue, 23(7), 575-586.

[40]E.J.M.Hiensch, A.Kapoor, B.L.Josefson[c], J.W.Ringsberg, J.C.O NielsenandF.J.Franklin[b]Two-Material Rail Development to Prevent Rolling Contact Fatigue and toReduce Noise Levels in Curved Rail Track

[41] MunidasaWidhana, Investigation of Surface Ratchetting due to Rail/Wheel Contact, Doctoral thesis, 2013.

[42] Fracture MechanicsTheory and ApplicationsBy,MajidMirzaei

Dedication

To my beloved mom, for her immeasurable love, encouragement, and patience